THE MODELLING OF ACCRETION DRIVEN PLASMA INSTABILITIES IN THE ACCRETION COLUMNS OF POLARS USING PLUTO

PRESENTED BY MR JPQ KHUMALO AT THE UNIVERSITY OF THE FREE STATE.

OVERSEEN BY PROF. PJ MEINTJES AND MR. IP VAN DER WESTHUIZEN

Funded by the University of the Free State Research Department & the National Research Foundation of the Republic of South Africa.

National Research Foundation

UNIVERSITY OF THE FREE STATE
UNIVERSITEIT VAN DIE VRYSTAAT
YUNIVESITHI YA FREISTATA
UFS

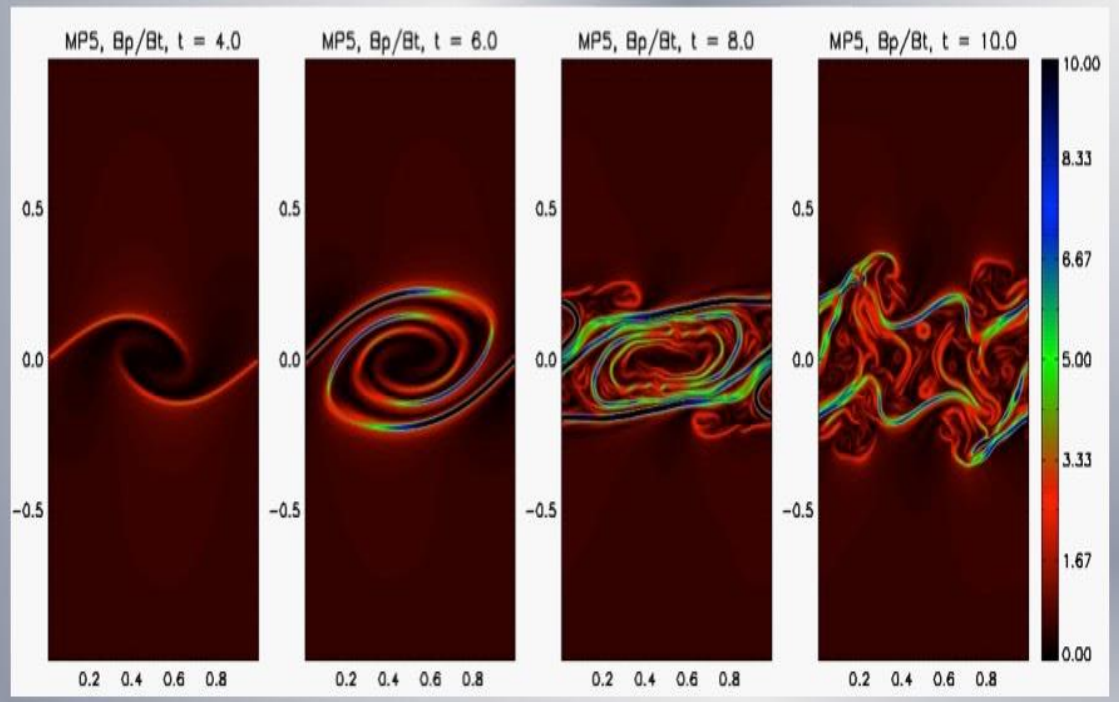

Ratio between poloidal and toroidal magnetic field components in a 2D planar Kelvin-Helmholtz instability between two magnetized fluids with relative Mach number 1 and Alfven speed 1/10. The finite-difference MPI5 scheme is used for this simulation. Mignone et al. JCP (2010) 229, 5896.

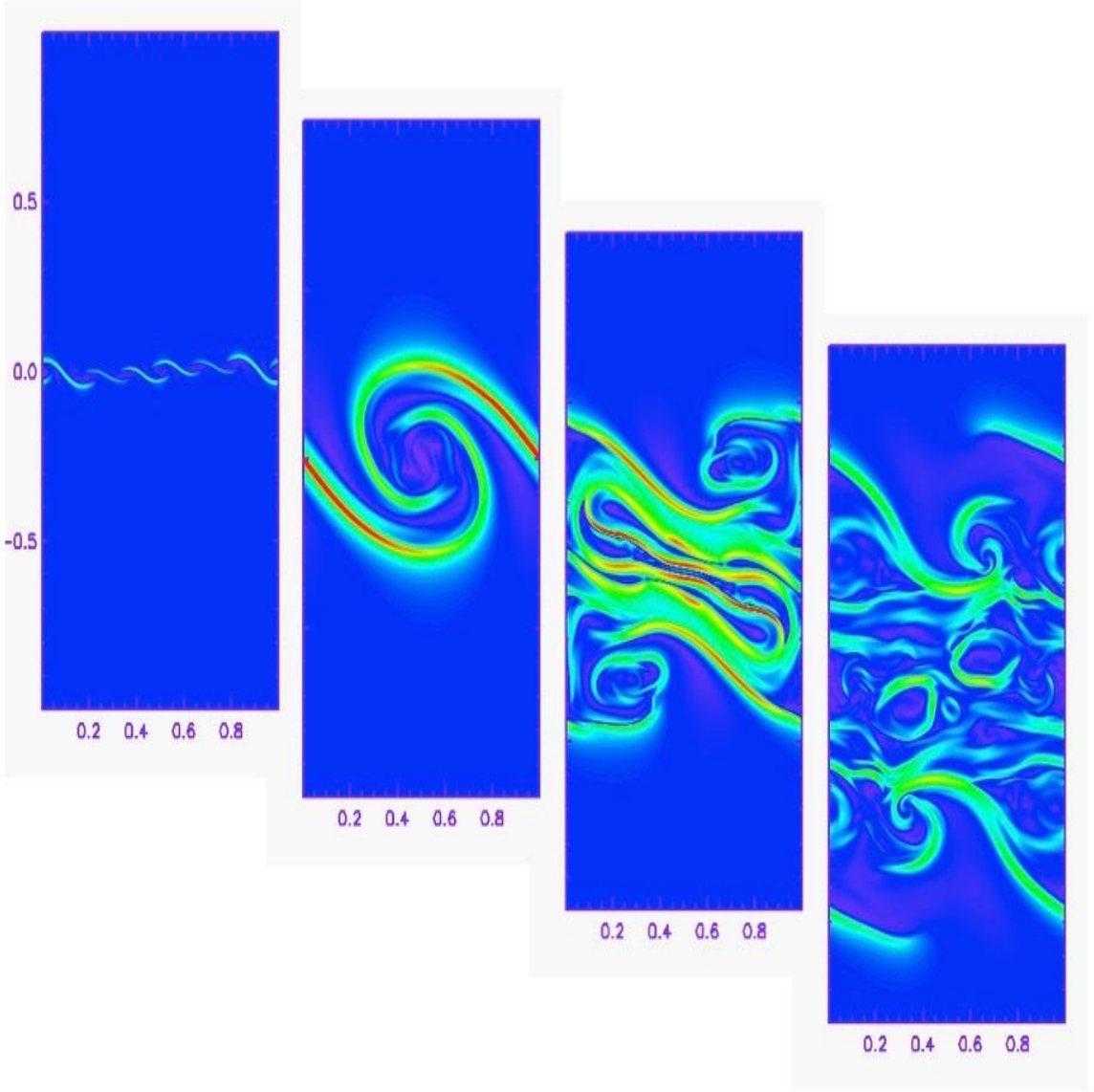

TIME

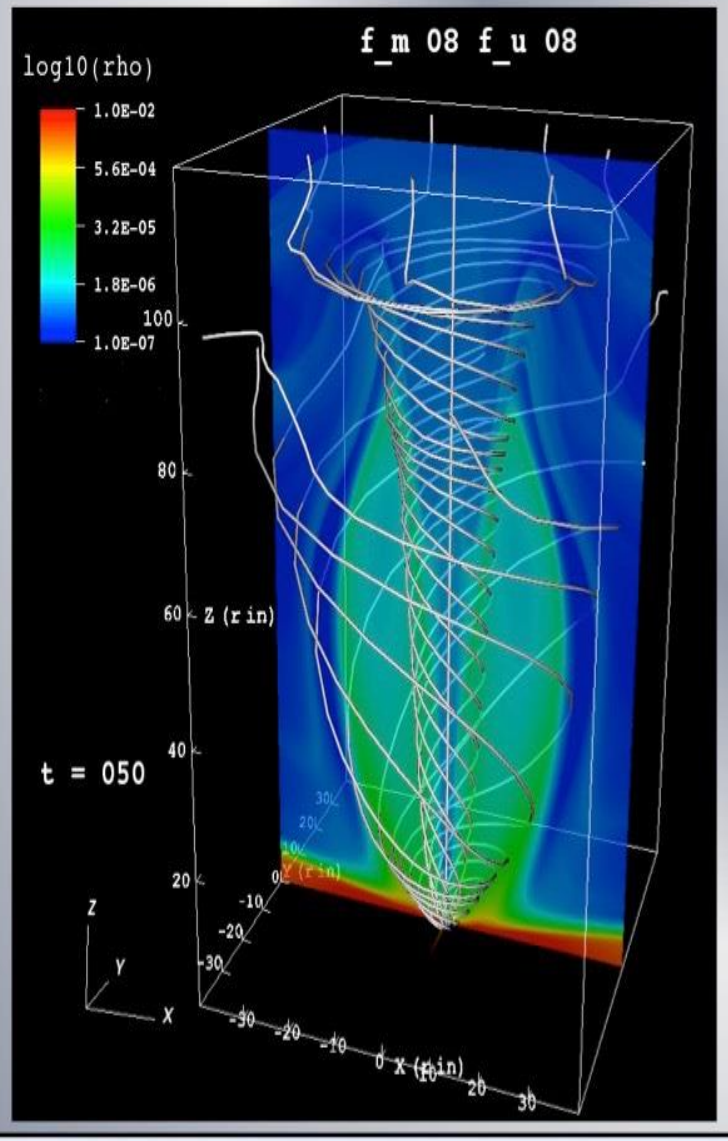

Jet ejection from a Keplerian accretion disc (Tzeferacos et al. 2012) Three dimensional rendering of the magnetic field superposed onto a 2D figure of the density logarithm. The outflow is magneto-centrifugally driven.

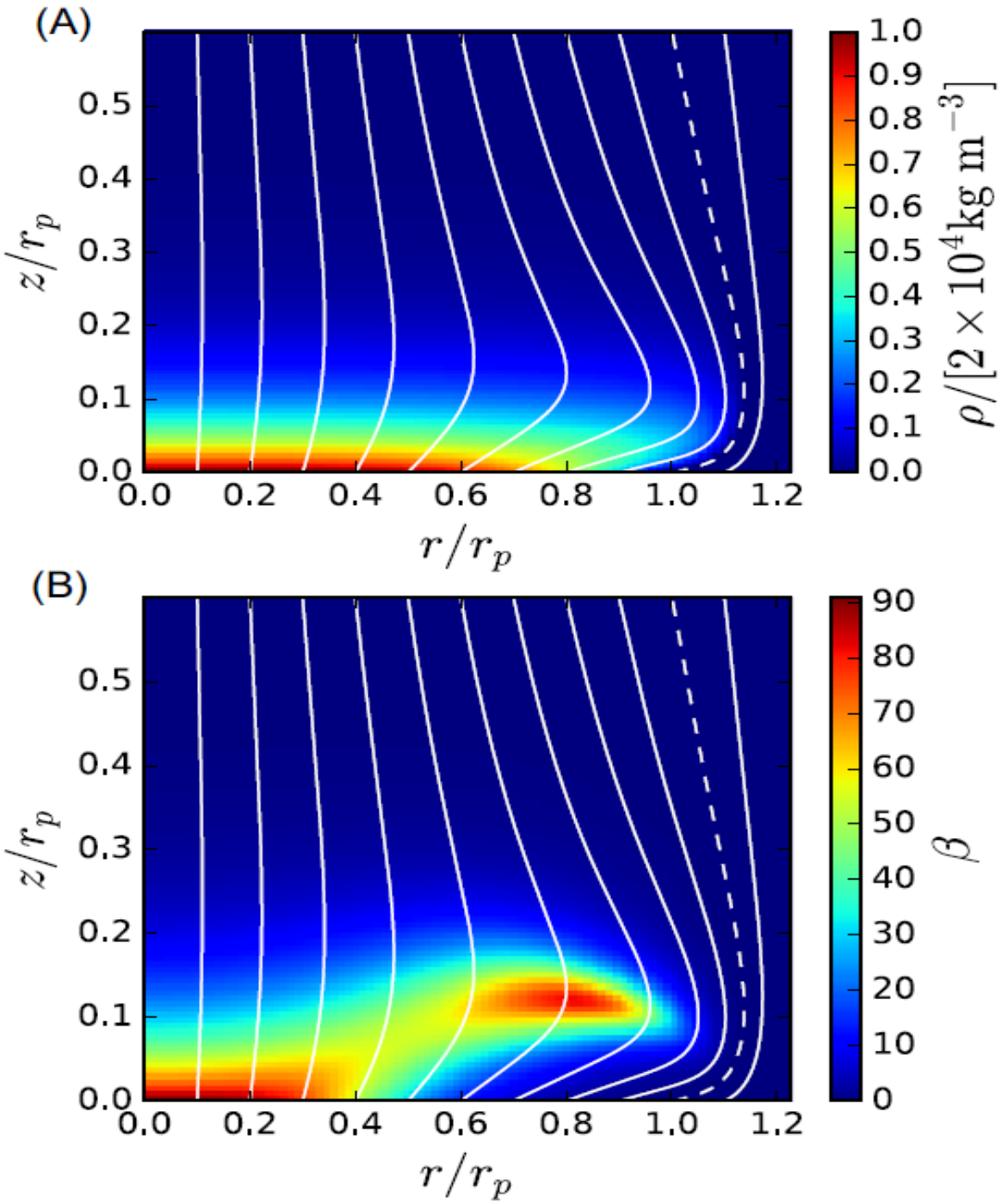

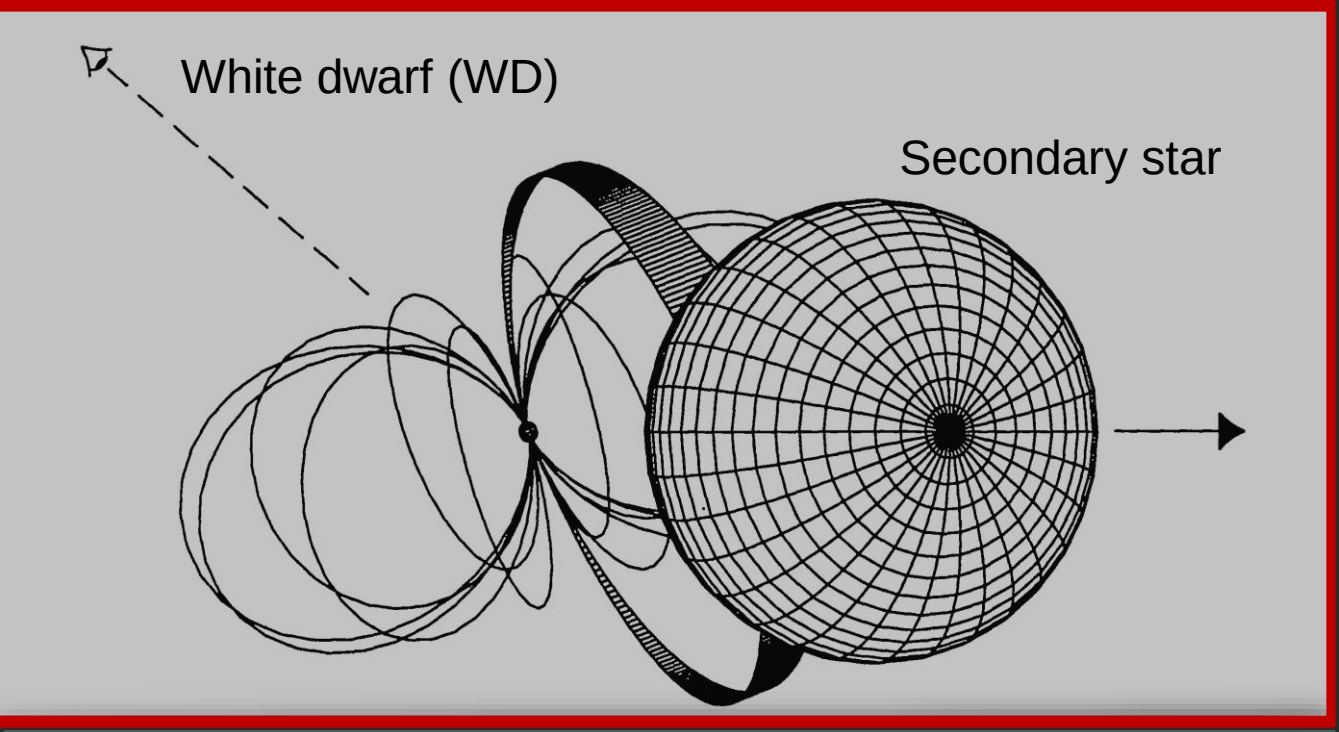

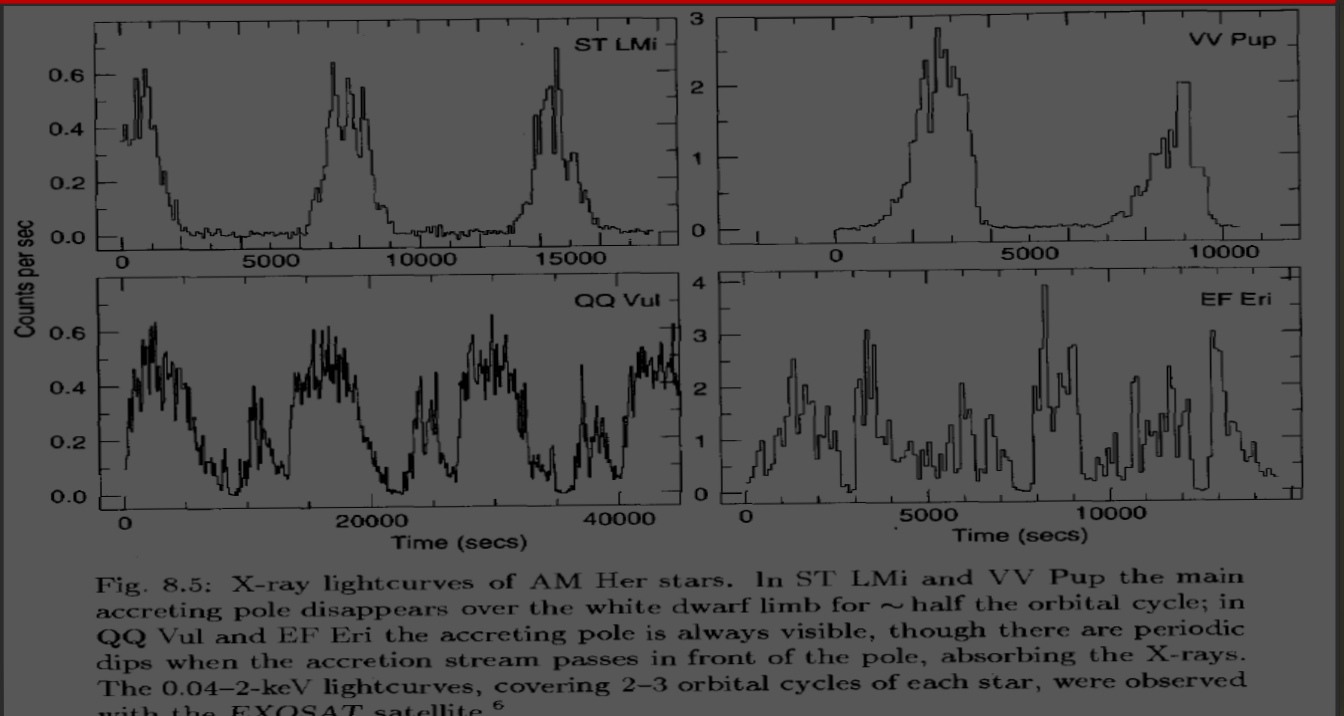

Fig. 8.5: X-ray lightcurves of AM Her stars. In ST LMi and VV Pup the main accreting pole disappears over the white dwarf limb for ~ half the orbital cycle; in QQ Vul and EF Eri the accreting pole is always visible, though there are periodic dips when the accretion stream passes in front of the pole, absorbing the X-rays. The 0.04–2-keV lightcurves, covering 2–3 orbital cycles of each star, were observed with the EXOSAT satellite.[6]

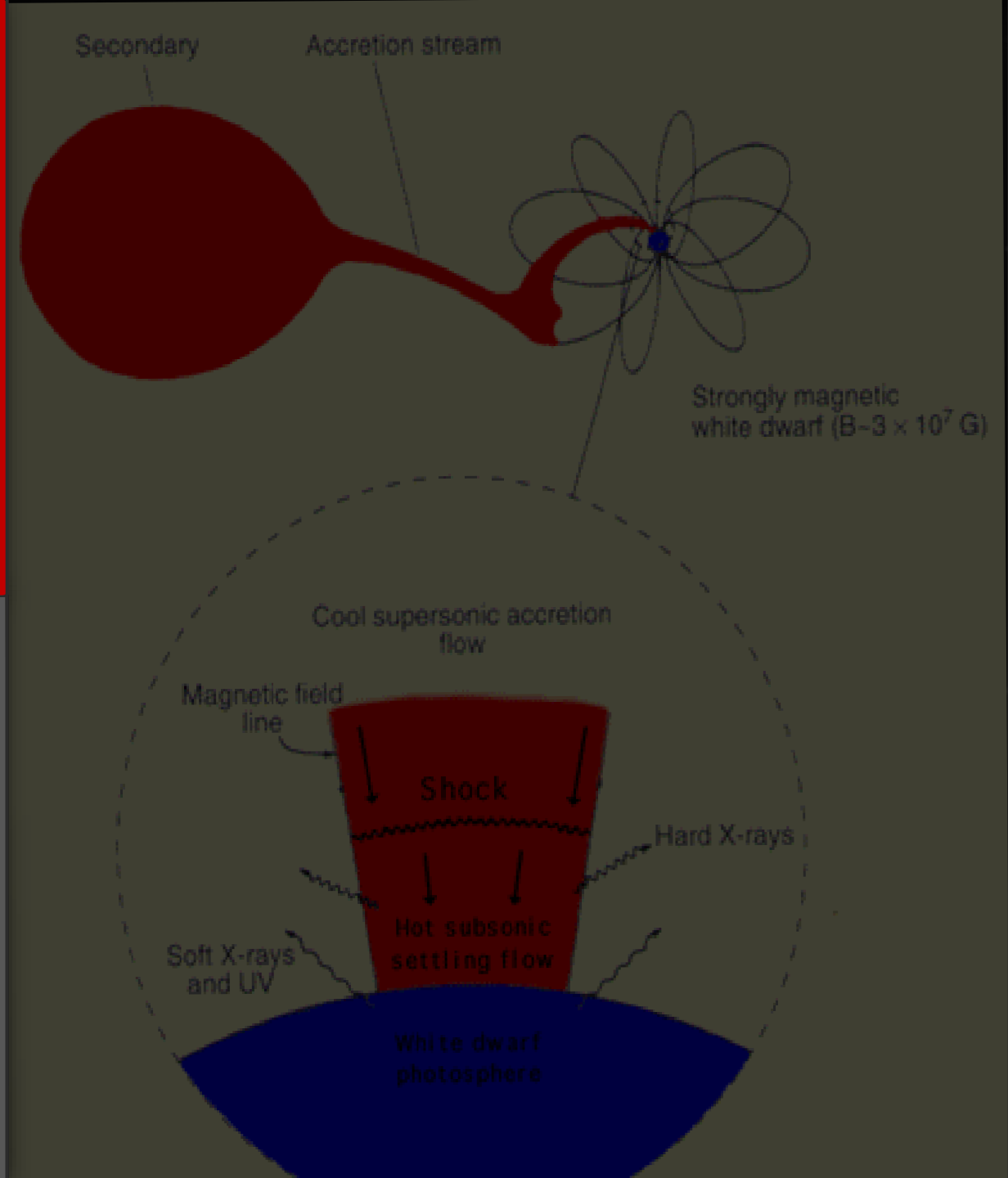

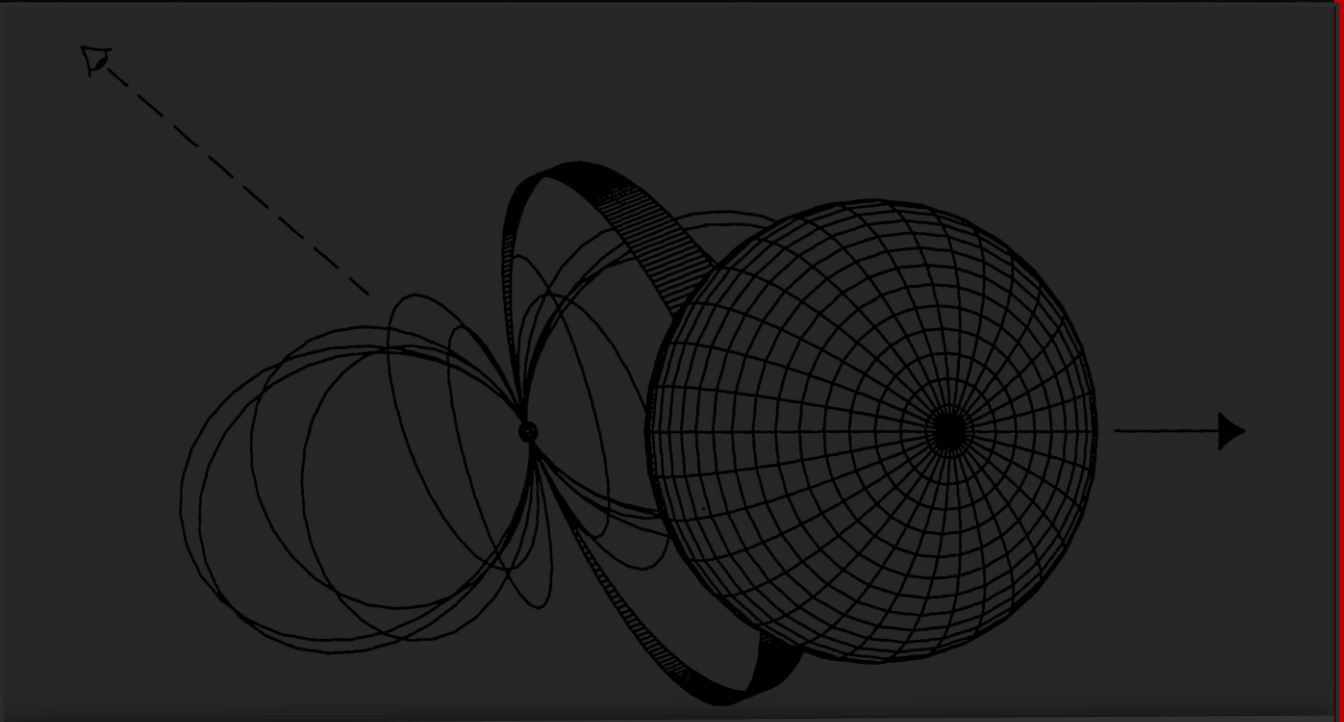

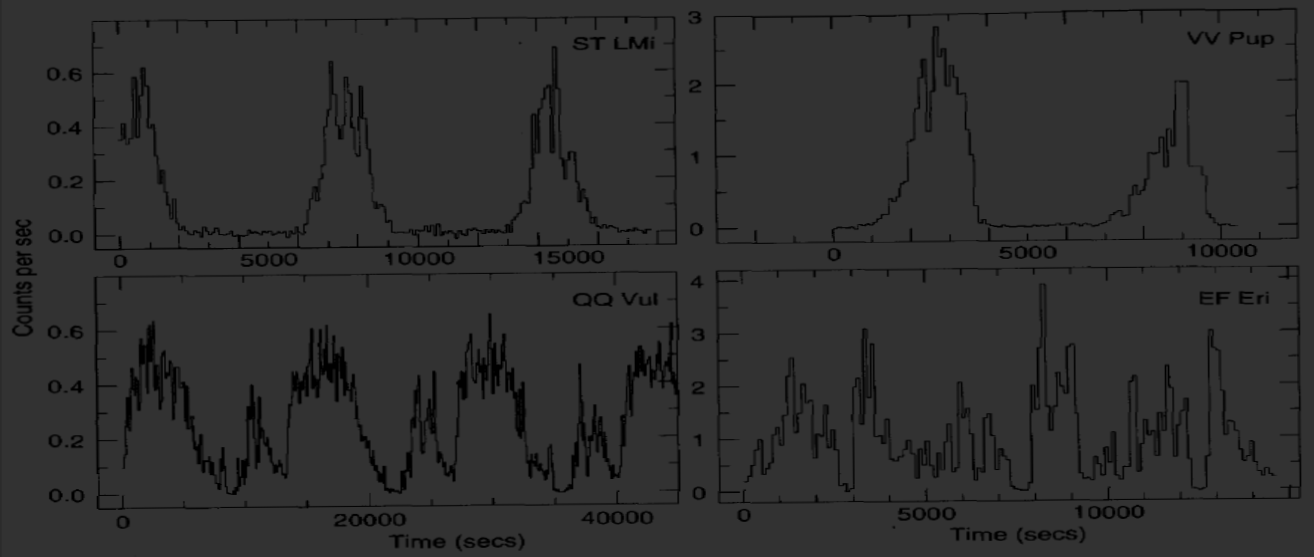

Fig. 8.5: X-ray lightcurves of AM Her stars. In ST LMi and VV Pup the main accreting pole disappears over the white dwarf limb for ~half the orbital cycle; in QQ Vul and EF Eri the accreting pole is always visible, though there are periodic dips when the accretion stream passes in front of the pole, absorbing the X-rays. The 0.04–2-keV lightcurves, covering 2–3 orbital cycles of each star, were observed with the EXOSAT satellite.[6]

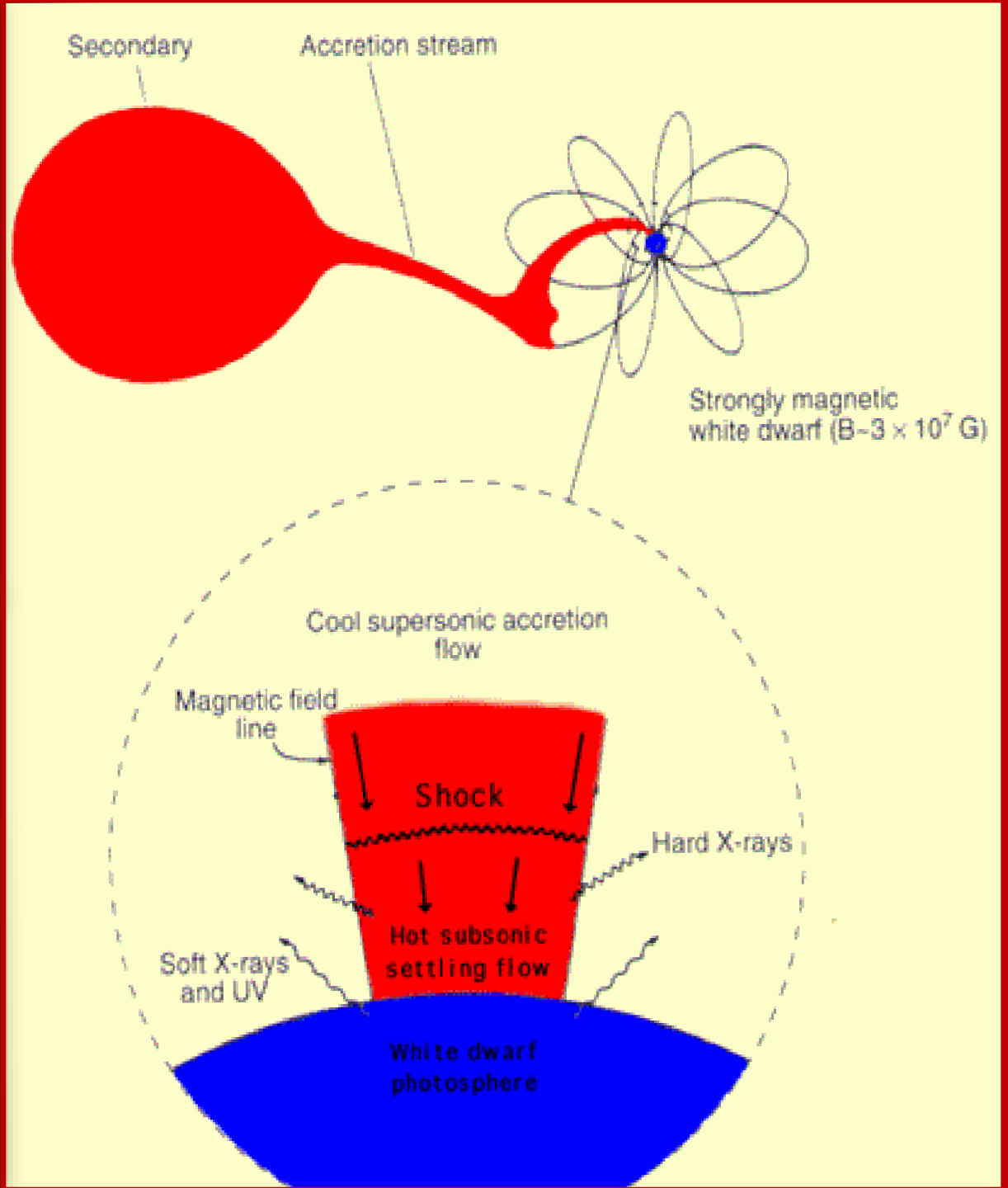

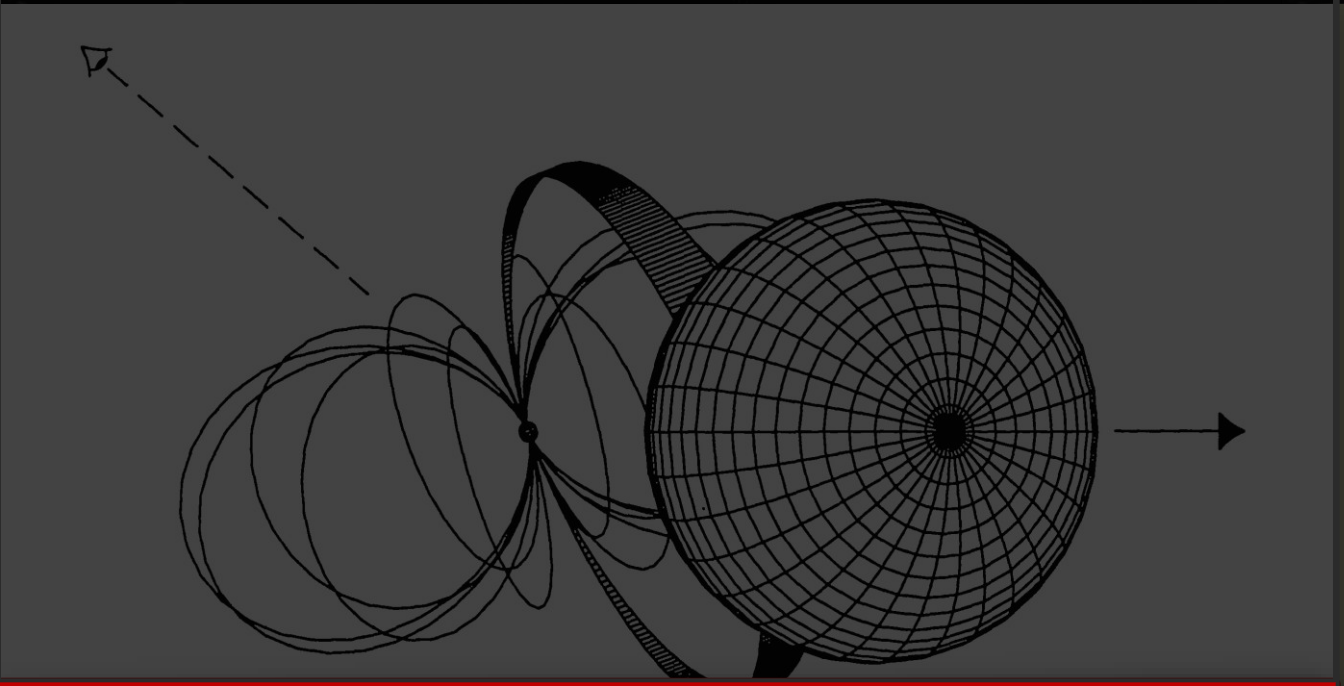

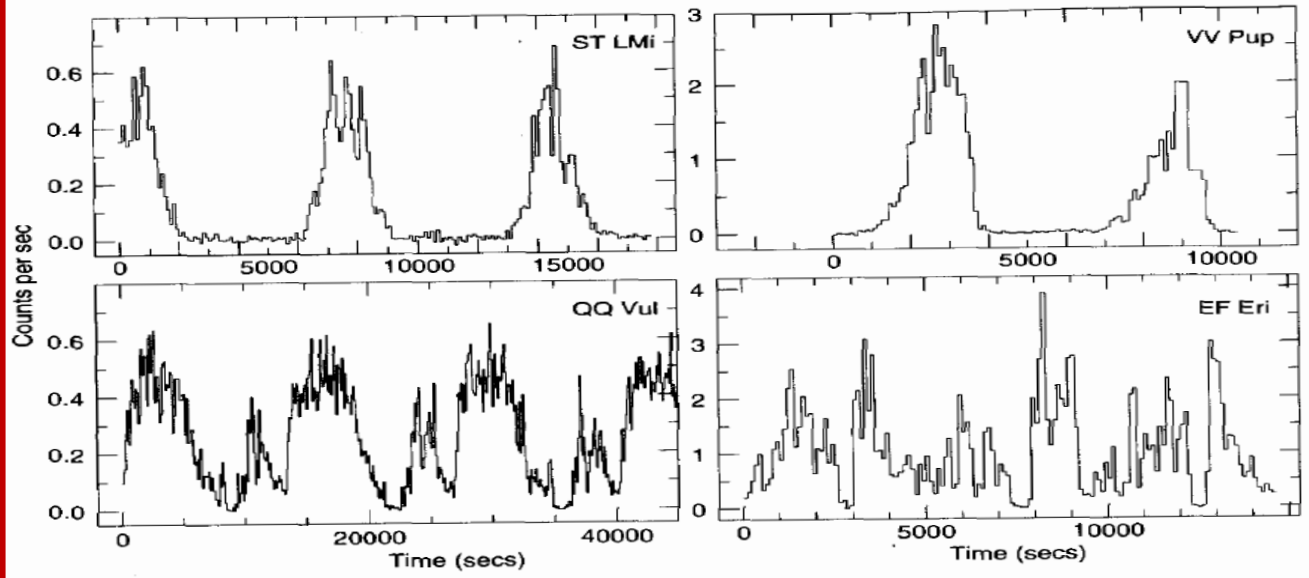

Fig. 8.5: X-ray lightcurves of AM Her stars. In ST LMi and VV Pup the main accreting pole disappears over the white dwarf limb for ~ half the orbital cycle; in QQ Vul and EF Eri the accreting pole is always visible, though there are periodic dips when the accretion stream passes in front of the pole, absorbing the X-rays. The 0.04–2-keV lightcurves, covering 2–3 orbital cycles of each star, were observed with the EXOSAT satellite.[6]

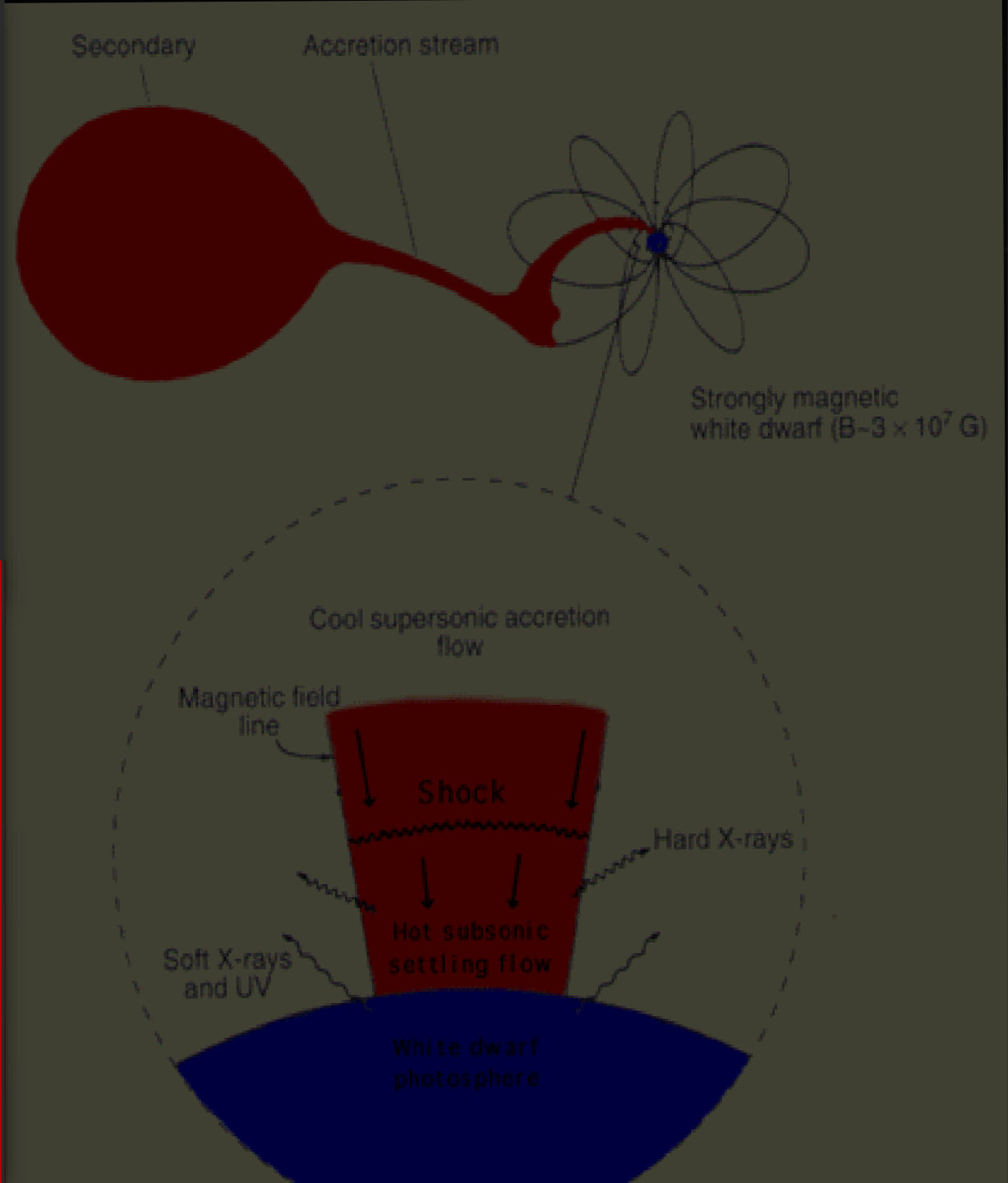

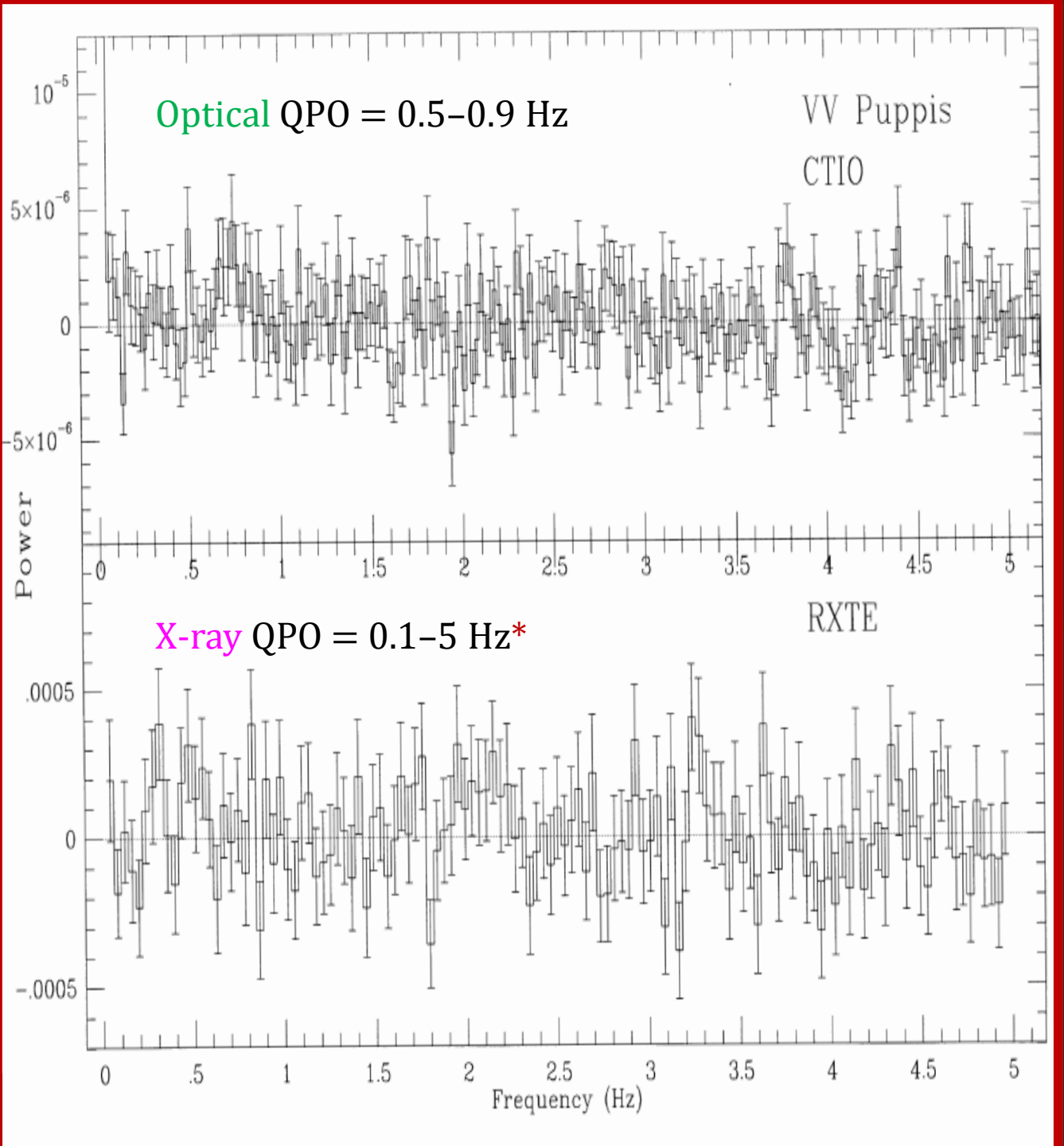
Optical QPO = 0.5–0.9 Hz
VV Puppis
CTIO
X-ray QPO = 0.1–5 Hz*
RXTE
Power
Frequency (Hz)

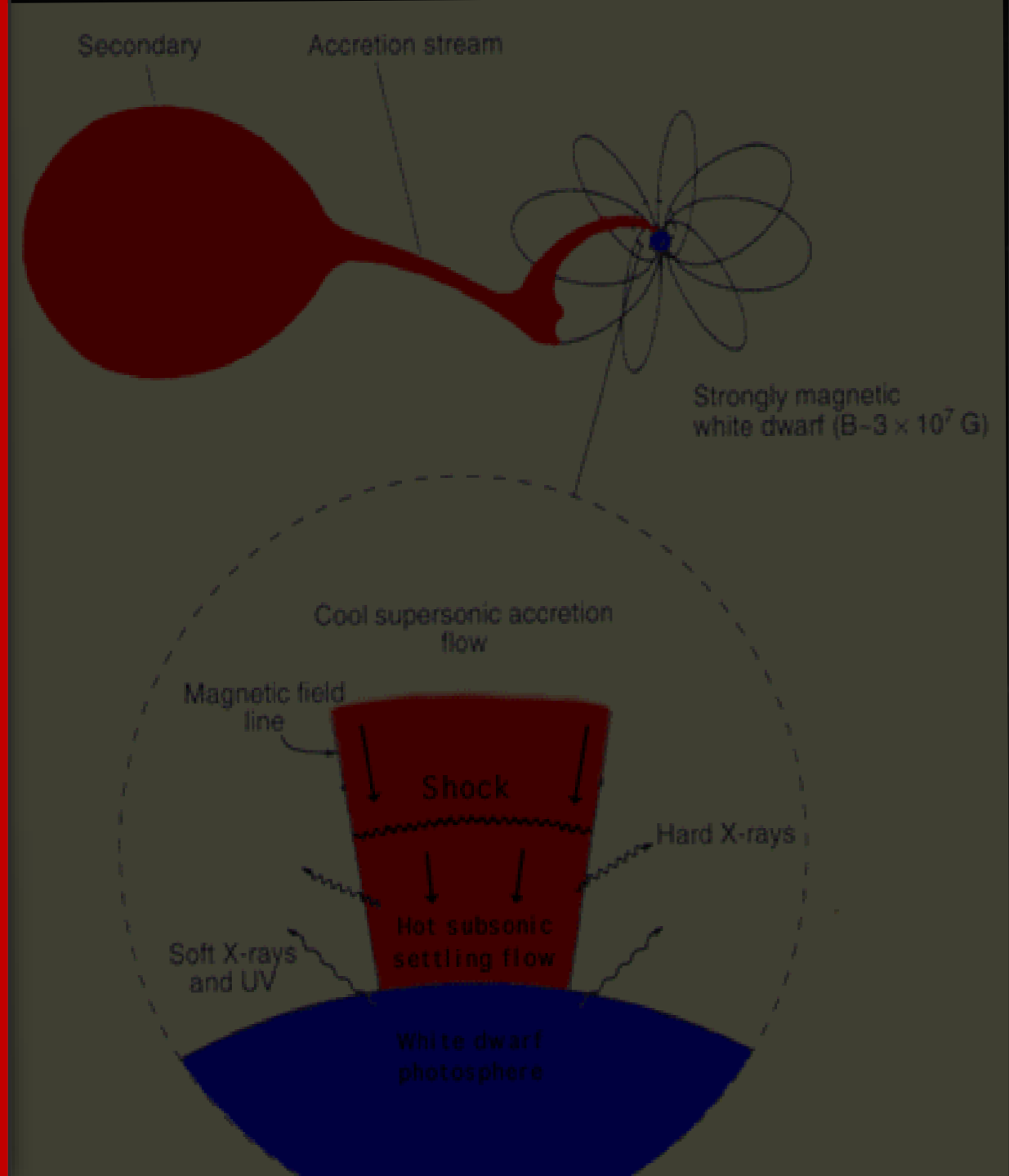
Secondary
Accretion stream
Strongly magnetic white dwarf (B~3 × 10^7 G)
Cool supersonic accretion flow
Magnetic field line
Shock
Hard X-rays
Hot subsonic settling flow
Soft X-rays and UV
White dwarf photosphere

Quantity	Value
Mass of WD	9.945e32 g
Radius of WD	1e9 cm
Specific mass accretion rate	$4\ \frac{g}{cm^2 s}$
Initial Density	$7.36e\text{-}09\ \frac{g}{cm^3}$
Initial Temperature	5e8 K
Initial Velocity	$5e6\ \frac{cm}{s}$
Initial Pressure	3.058e8 Barye

Table 1: Model white dwarf and in-plunging fluid parameters used in initial conditions of *PLUTO* simulation.

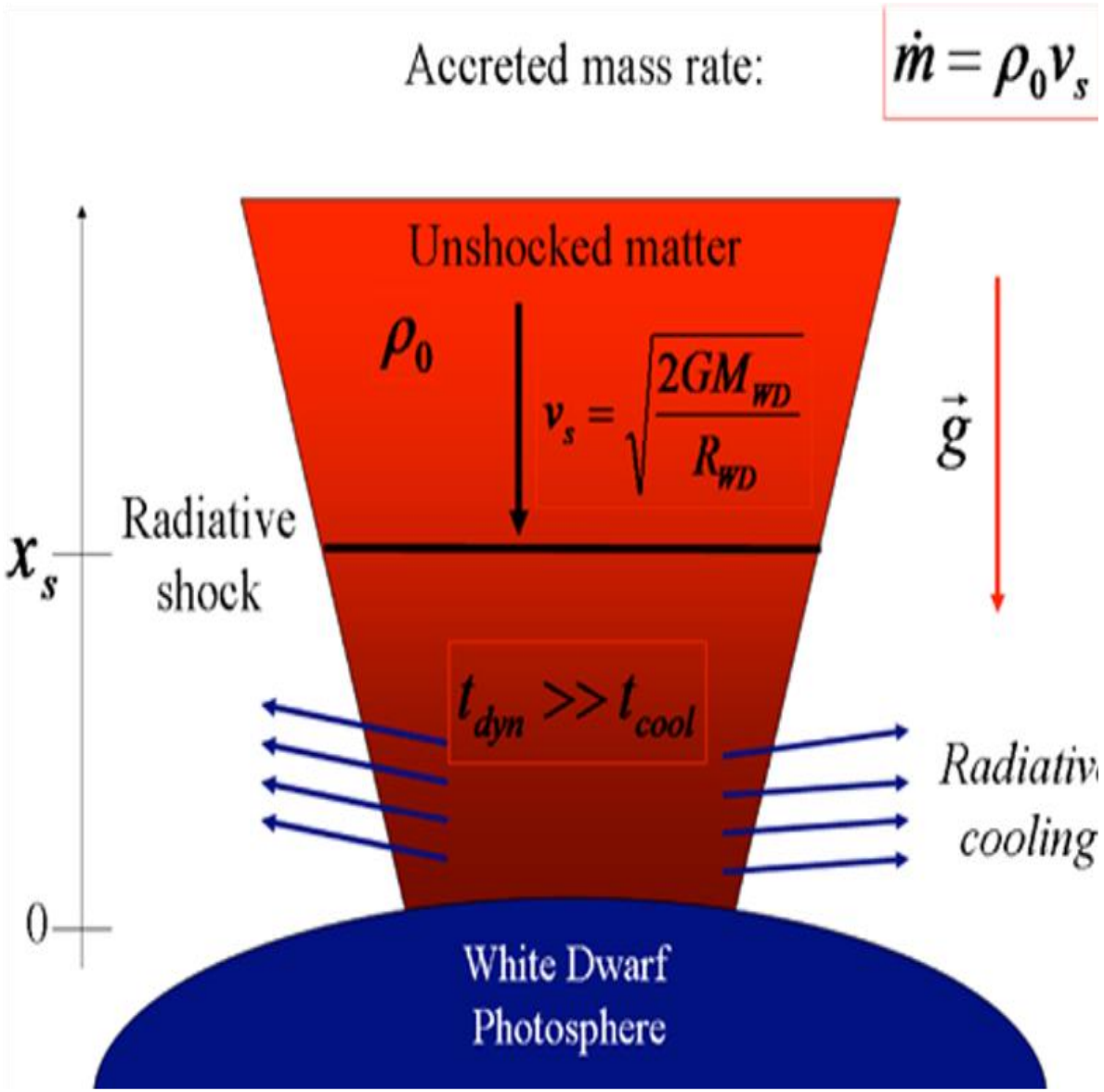
Accreted mass rate:
$\dot{m} = \rho_0 v_s$
Unshocked matter
ρ_0
$v_s = \sqrt{\frac{2GM_{WD}}{R_{WD}}}$
$\vec{g}$
x_s
Radiative shock
$t_{dyn} >> t_{cool}$
Radiativ
cooling
0
White Dwarf
Photosphere

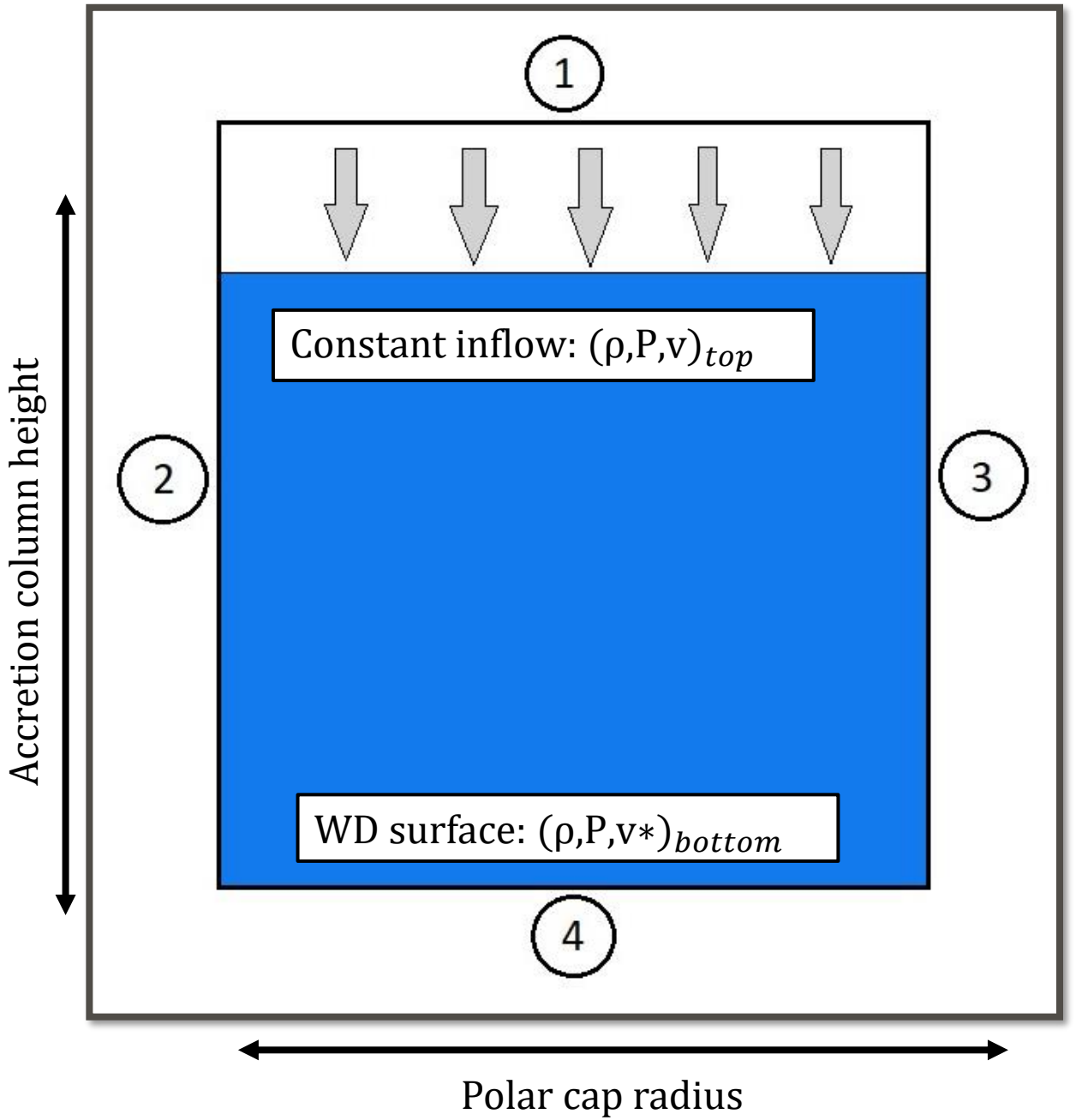
1
Constant inflow: (ρ,P,v)$_{top}$
2
3
WD surface: (ρ,P,v∗)$_{bottom}$
4
Accretion column height
Polar cap radius

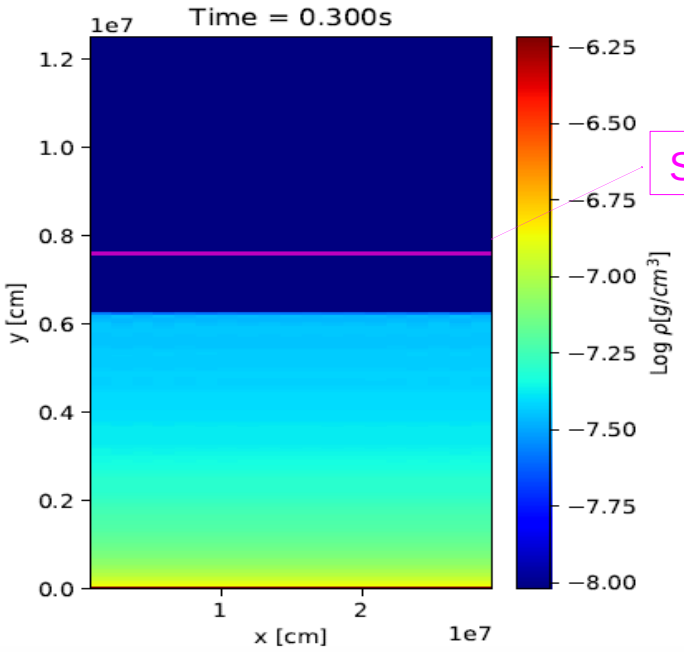

Shock height

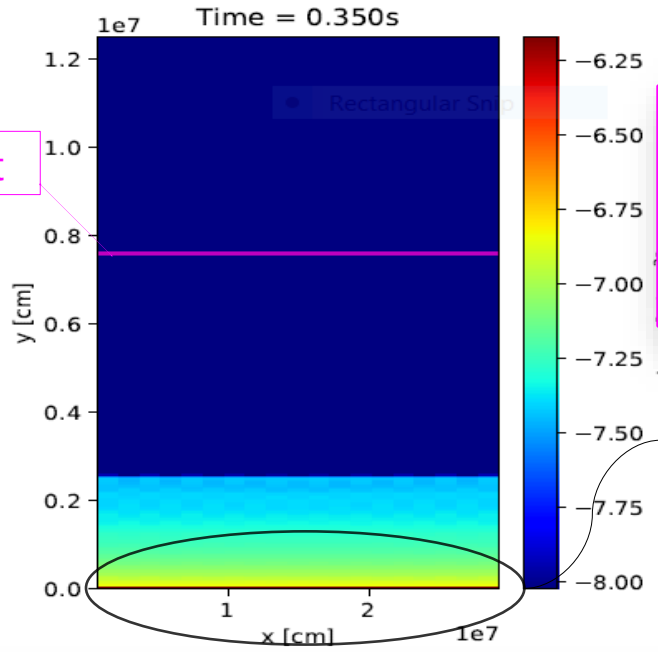

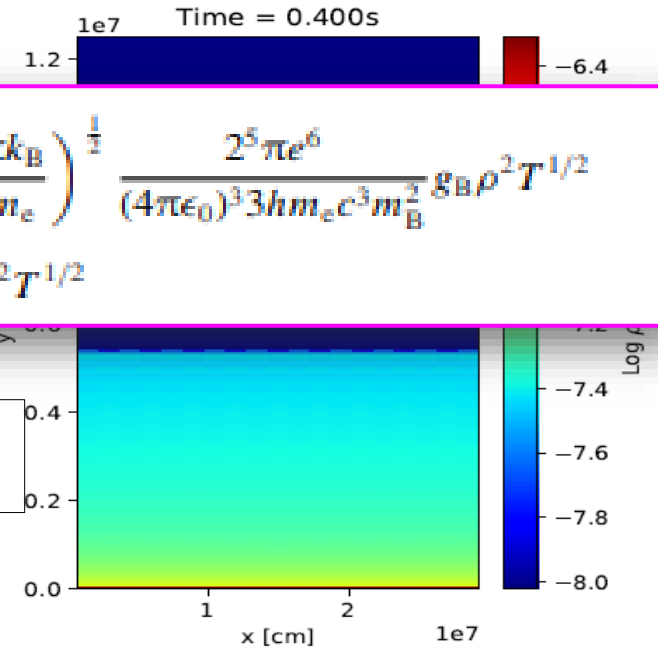

$$\Lambda_{\text{brem}} = \left(\frac{2\pi k_B}{3m_e}\right)^{\frac{1}{2}} \frac{2^5\pi e^6}{(4\pi\epsilon_0)^3 3hm_e c^3 m_B^2} g_B \rho^2 T^{1/2}$$
$$= \Lambda_0 \rho^2 T^{1/2}$$

Settling near surface

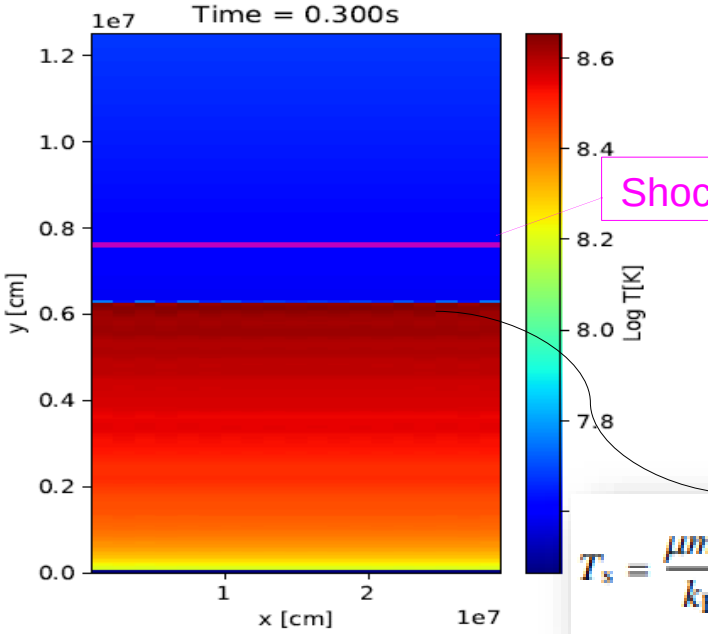

Shock height

$$T_s = \frac{\mu m_H}{k_B} \frac{2(\gamma-1)}{(\gamma+1)^2} v_{ff}^2$$

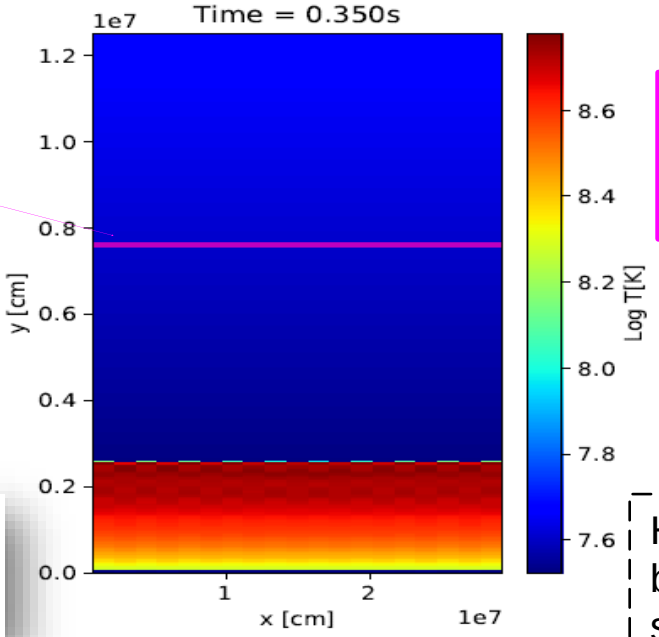

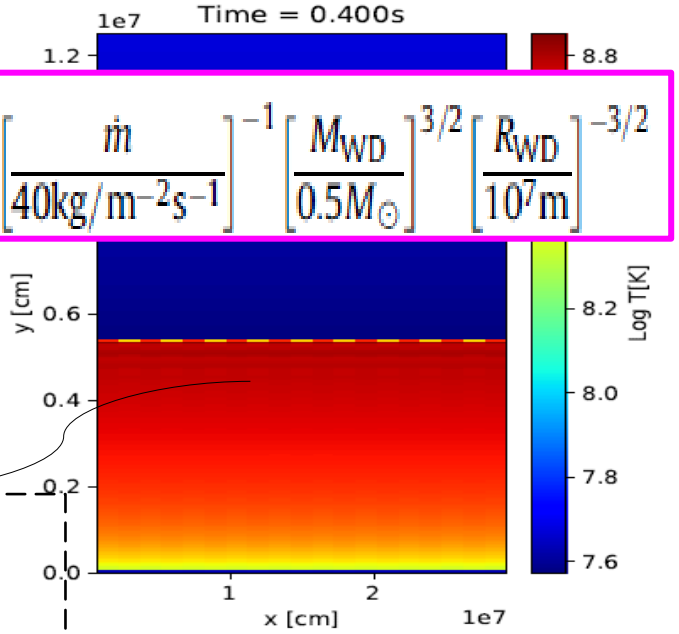

$$x_s = 7.6\times10^4 \text{m} \left[\frac{\dot{m}}{40\text{kg/m}^{-2}\text{s}^{-1}}\right]^{-1} \left[\frac{M_{WD}}{0.5M_\odot}\right]^{3/2} \left[\frac{R_{WD}}{10^7\text{m}}\right]^{-3/2}$$

Hotter directly behind primary shock.

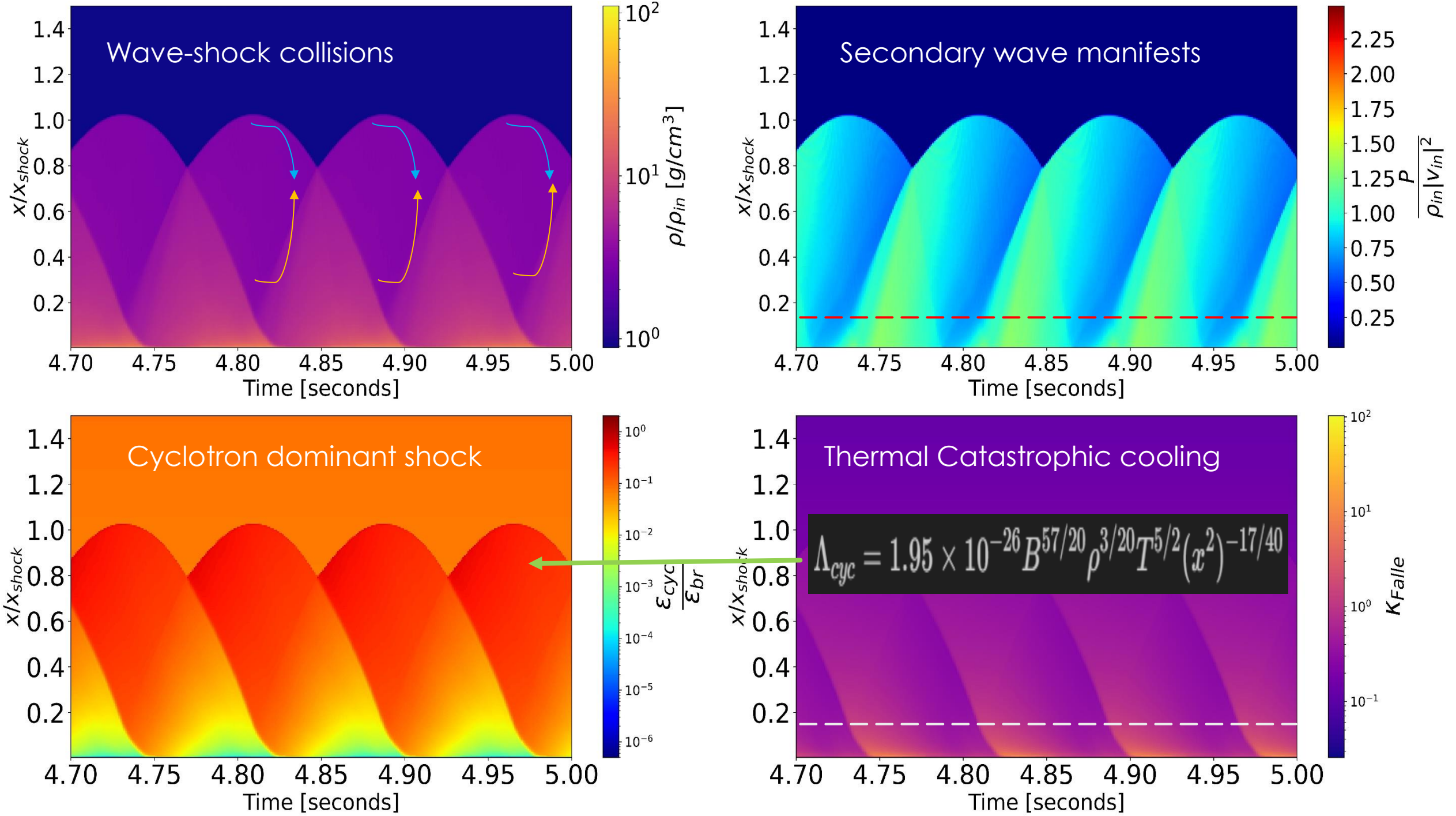
Wave-shock collisions
Secondary wave manifests
Cyclotron dominant shock
Thermal Catastrophic cooling
$\Lambda_{cyc} = 1.95 \times 10^{-26} B^{57/20} \rho^{3/20} T^{5/2} (x^2)^{-17/40}$
x/x_{shock}
Time [seconds]
ρ/ρ_{in} [g/cm^3]
$\frac{P}{\rho_{in}|v_{in}|^2}$
$\frac{\varepsilon_{cyc}}{\varepsilon_{br}}$
K_{Falle}

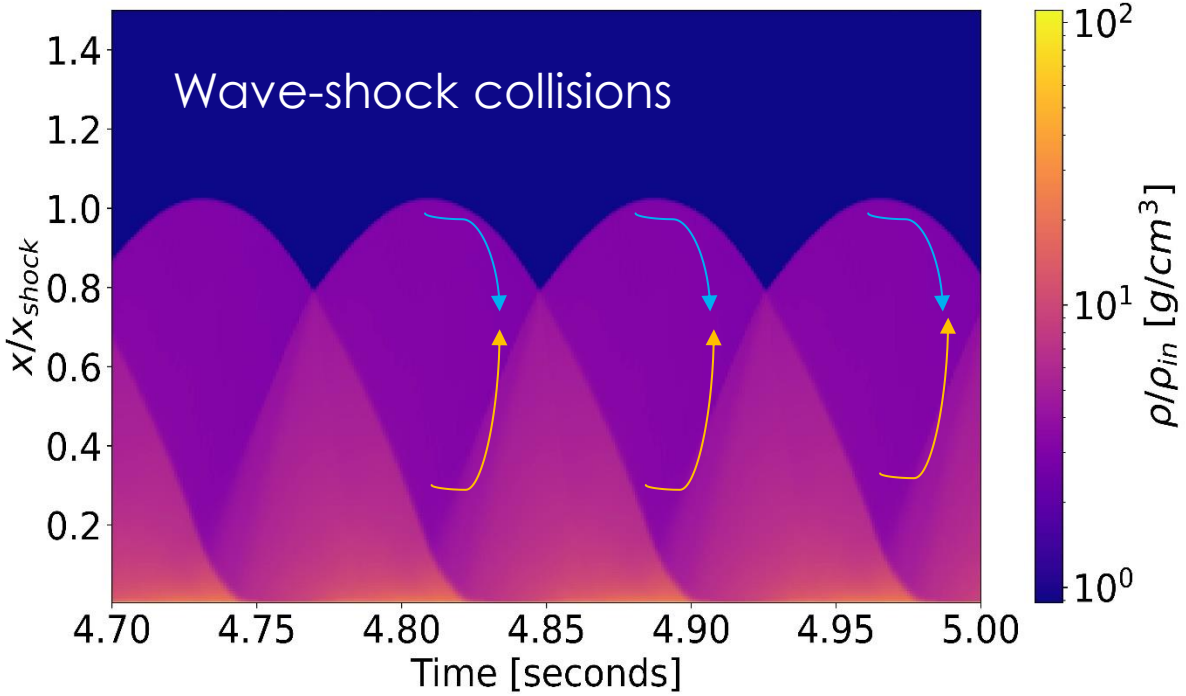
Wave-shock collisions
x/x_{shock}
Time [seconds]
ρ/ρ_{in} [g/cm^3]

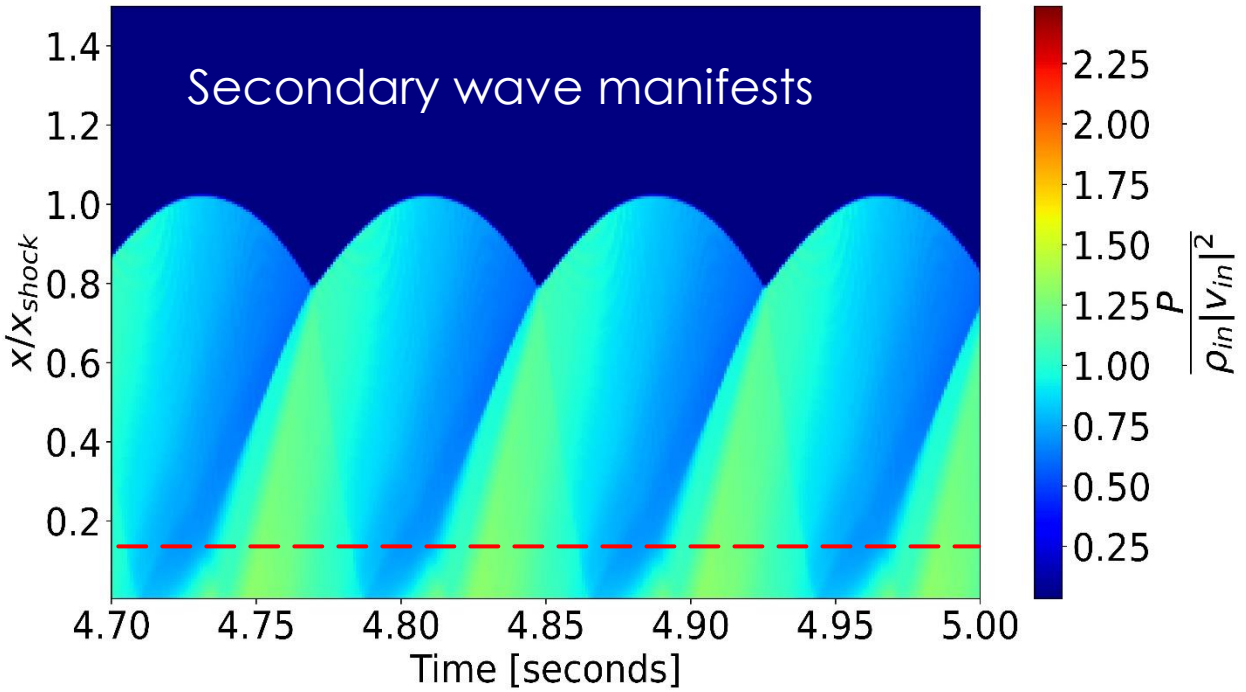
Secondary wave manifests
x/x_{shock}
Time [seconds]
$\frac{P}{\rho_{in}|v_{in}|^2}$

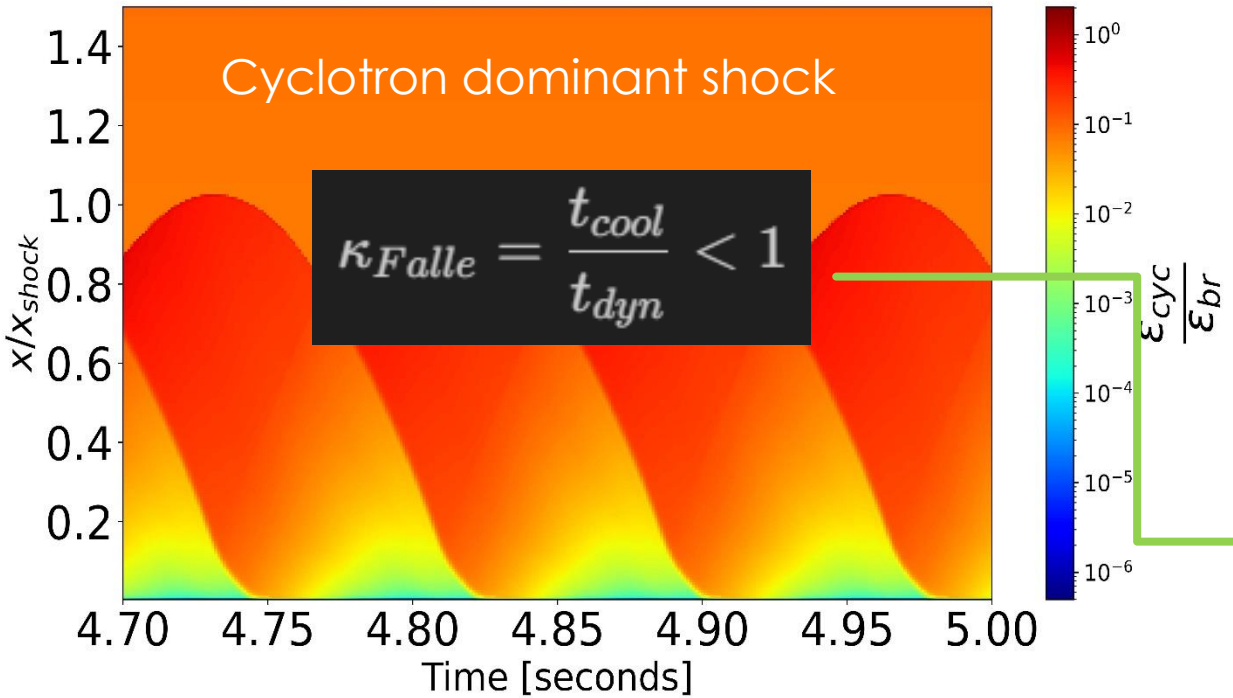
Cyclotron dominant shock
$\kappa_{Falle} = \frac{t_{cool}}{t_{dyn}} < 1$
x/x_{shock}
Time [seconds]
$\frac{\varepsilon_{cyc}}{\varepsilon_{br}}$

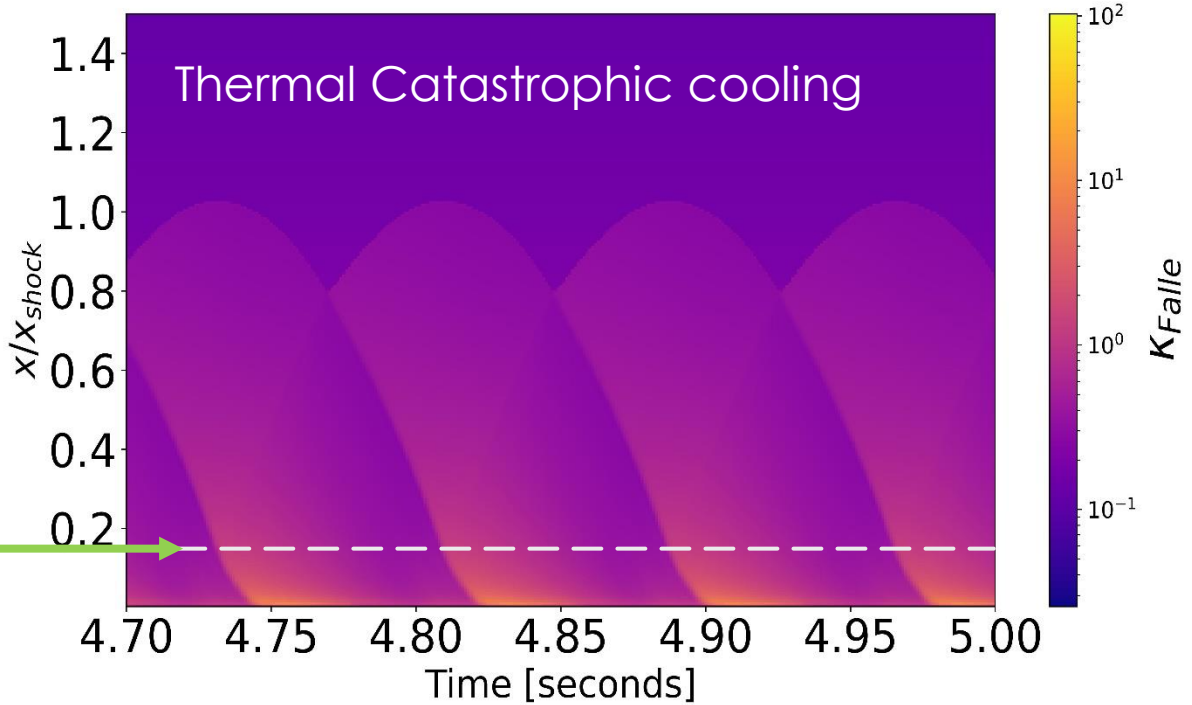
Thermal Catastrophic cooling
x/x_{shock}
Time [seconds]
κ_{Falle}

$$\Lambda_{\rm cycl} = 5.7 \times 10^{6} \,{\rm erg\ cm^{-3}\ s^{-1}} \left(\frac{\rho}{4 \times 10^{-8}\ {\rm g\ cm^{-3}}}\right)^{\frac{3}{20}} \times \left(\frac{x^2}{10^{15}\ {\rm cm^2}}\right)^{\frac{-17}{40}} \left(\frac{T}{10^{8}\ {\rm K}}\right)^{\frac{5}{2}} \left(\frac{B}{10\ {\rm MG}}\right)^{\frac{57}{20}}$$

$$\Lambda_{\rm brem} = \left(\frac{2\pi k_{\rm B}}{3 m_{\rm e}}\right)^{\frac{1}{2}} \frac{2^5 \pi e^6}{(4\pi\epsilon_0)^3 3 h m_{\rm e} c^3 m_{\rm B}^2} g_{\rm B} \rho^2 T^{1/2} = \Lambda_0 \rho^2 T^{1/2}$$

Secondary wave

Primary shock

INFLOWING MATTER

$j_{\nu_a}^{cyc} \in$ Log[-7.82,-6.89]

$j_{\nu_a}^{br} \in$ Log[-6.79,-6.04]

$\rho \in$ Log[-8.14,-6.49]

$T \in$ Log[7.64,8.58]

$\kappa_{Falle} \in$ Log[-1.59,0.26]

$x_{ac} \simeq 0.11\, x_{s_1}$

$x_{s_1} \simeq 76 \times 10^5$ cm

Normalised Value

10^1

10^0

10^{-1}

0.0 0.2 0.4 0.6 0.8 1.0 1.2

$\left(\frac{x}{x_s^{Aizu}}\right)$

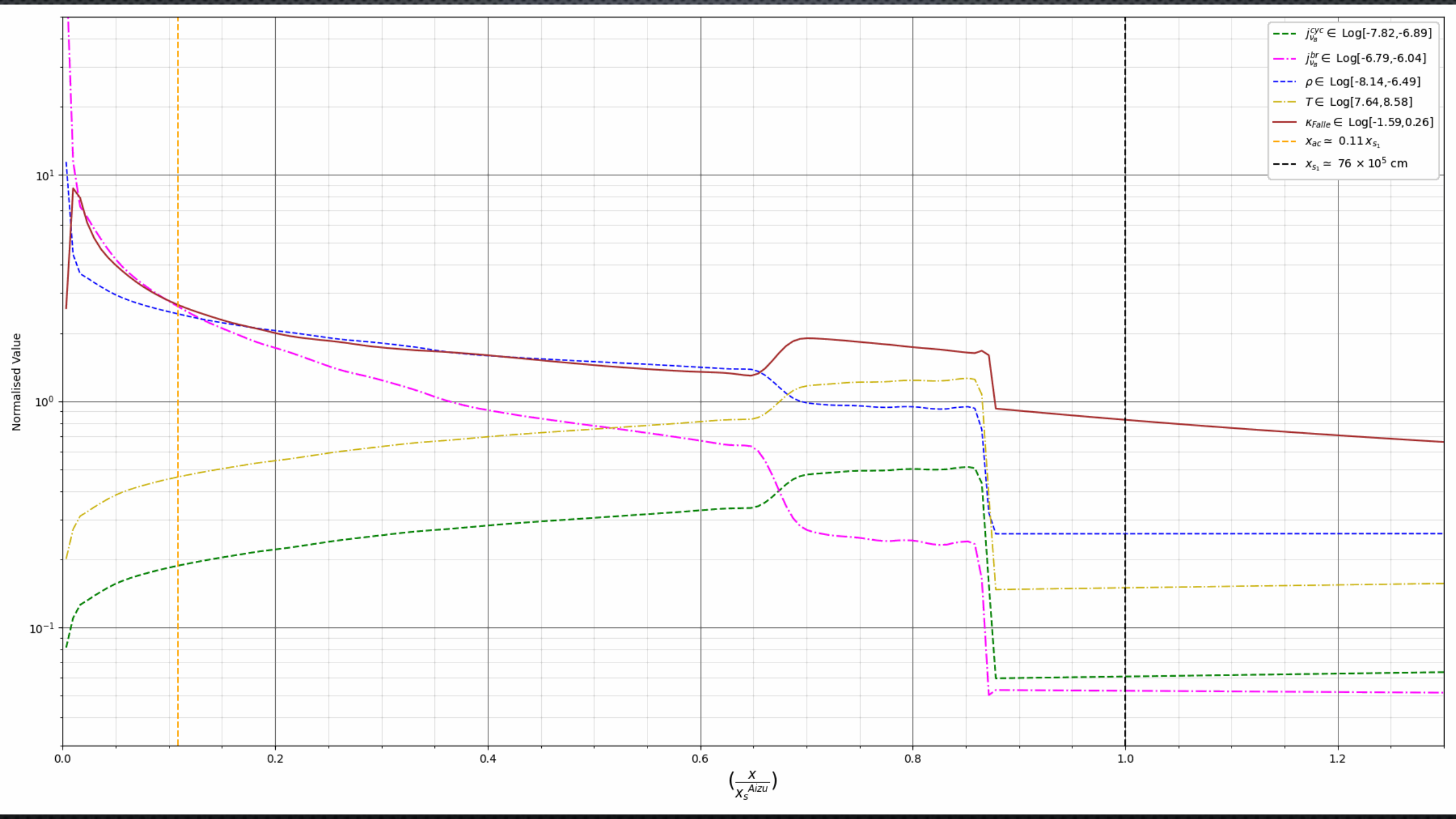
$j^{cyc}_{\nu_B} \in$ Log[-7.82,-6.89]
$j^{br}_{\nu_B} \in$ Log[-6.79,-6.04]
$\rho \in$ Log[-8.14,-6.49]
$T \in$ Log[7.64,8.58]
$\kappa_{Falle} \in$ Log[-1.59,0.26]
$x_{ac} \simeq 0.11\, x_{s_1}$
$x_{s_1} \simeq 76 \times 10^5$ cm
Normalised Value
10^1
10^0
10^{-1}
0.0
0.2
0.4
0.6
0.8
1.0
1.2
$\left(\frac{x}{x_s^{Aizu}}\right)$

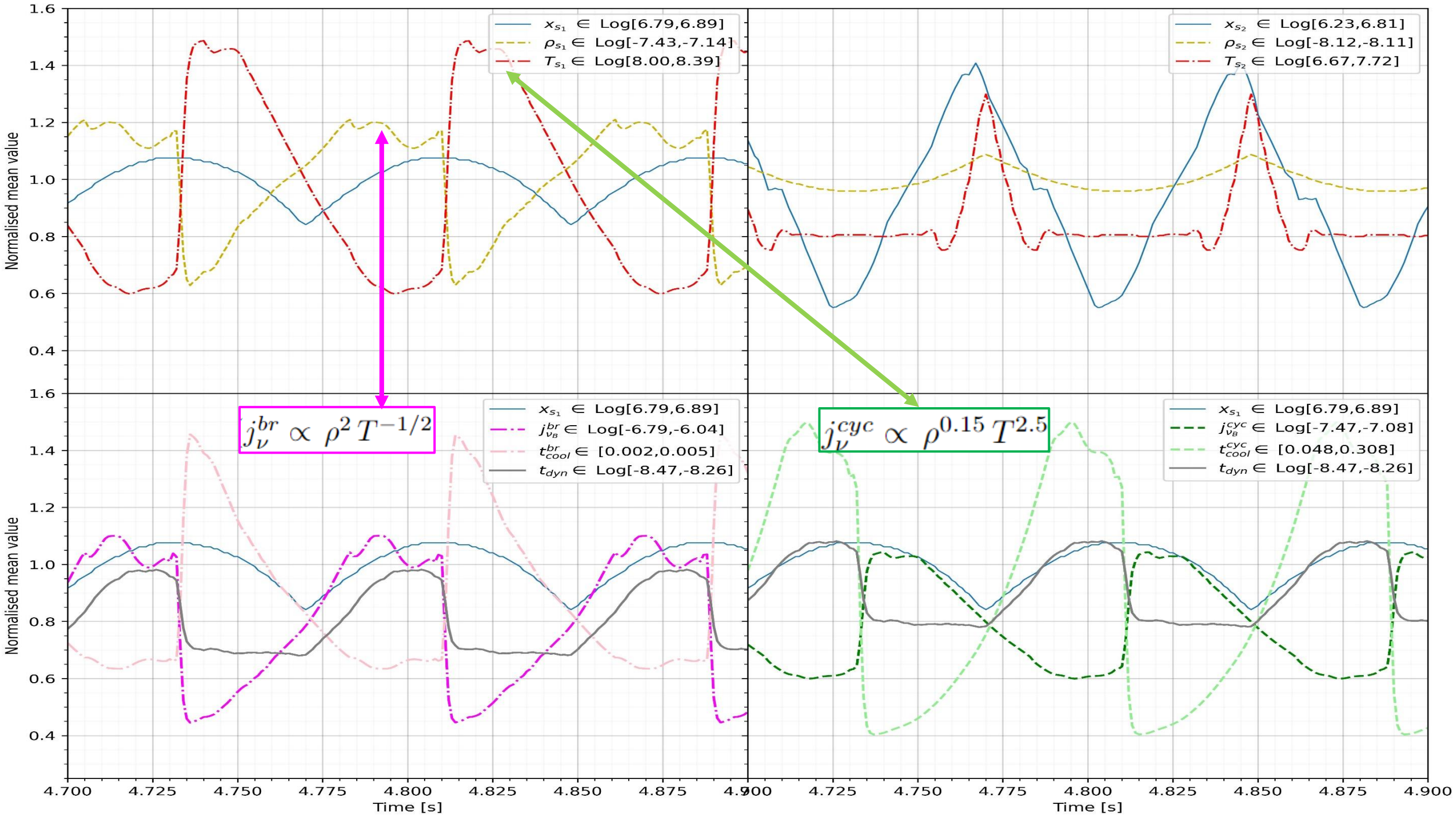
$x_{s_1} \in$ Log[6.79,6.89]
$\rho_{s_1} \in$ Log[-7.43,-7.14]
$T_{s_1} \in$ Log[8.00,8.39]
$x_{s_2} \in$ Log[6.23,6.81]
$\rho_{s_2} \in$ Log[-8.12,-8.11]
$T_{s_2} \in$ Log[6.67,7.72]
$j_\nu^{br} \propto \rho^2 T^{-1/2}$
$x_{s_1} \in$ Log[6.79,6.89]
$j_{\nu_B}^{br} \in$ Log[-6.79,-6.04]
$t_{cool}^{br} \in$ [0.002,0.005]
$t_{dyn} \in$ Log[-8.47,-8.26]
$j_\nu^{cyc} \propto \rho^{0.15} T^{2.5}$
$x_{s_1} \in$ Log[6.79,6.89]
$j_{\nu_B}^{cyc} \in$ Log[-7.47,-7.08]
$t_{cool}^{cyc} \in$ [0.048,0.308]
$t_{dyn} \in$ Log[-8.47,-8.26]
Normalised mean value
Normalised mean value
Time [s]
Time [s]

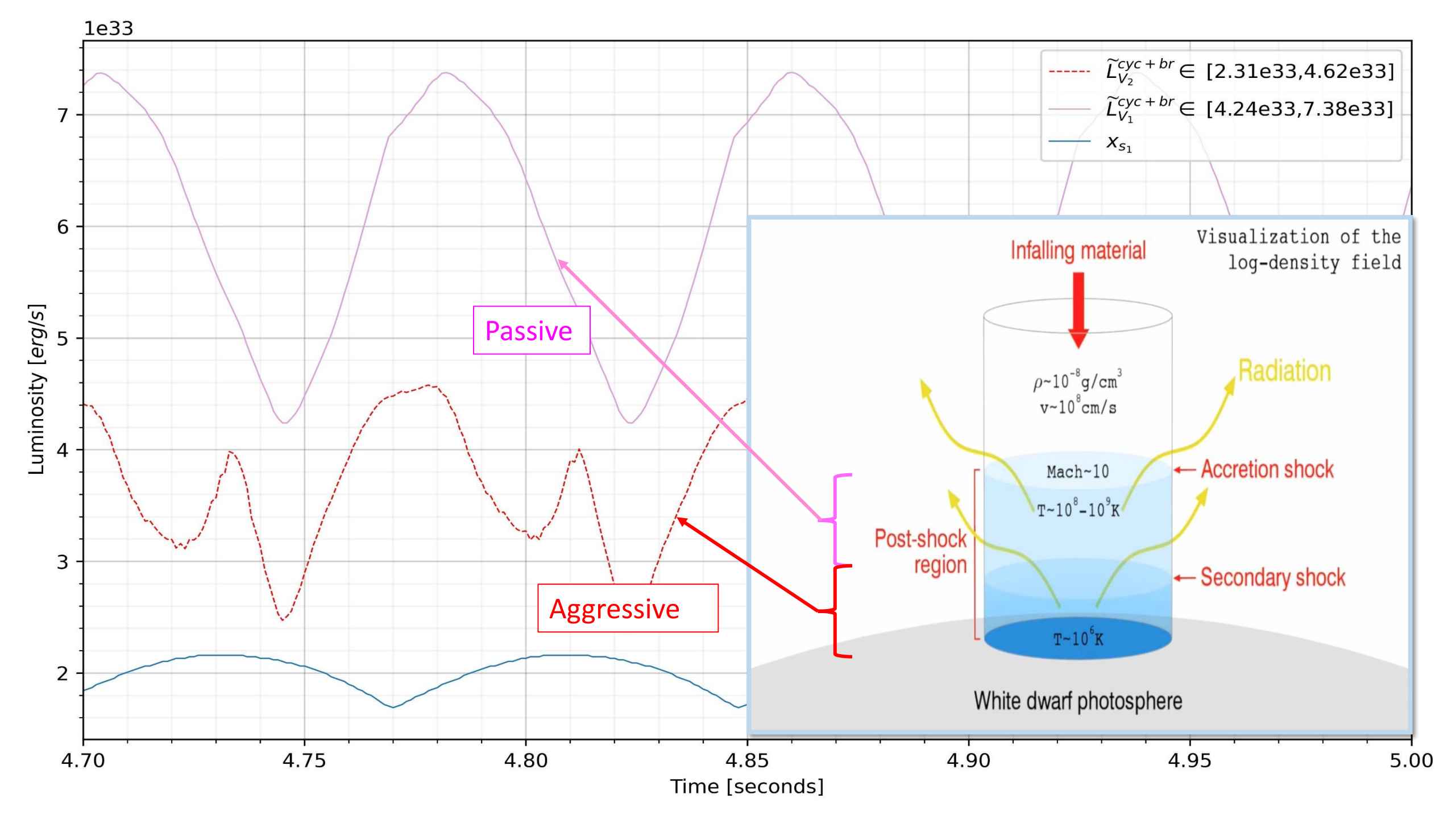
1e33
$\widetilde{L}_{V_2}^{cyc+br} \in$ [2.31e33,4.62e33]
$\widetilde{L}_{V_1}^{cyc+br} \in$ [4.24e33,7.38e33]
x_{s_1}
Passive
Aggressive
Luminosity [erg/s]
Time [seconds]
Visualization of the log-density field
Infalling material
ρ~10^{-8}g/cm^3
v~10^8cm/s
Radiation
Mach~10
Accretion shock
T~10^8-10^9K
Post-shock region
Secondary shock
T~10^6K
White dwarf photosphere

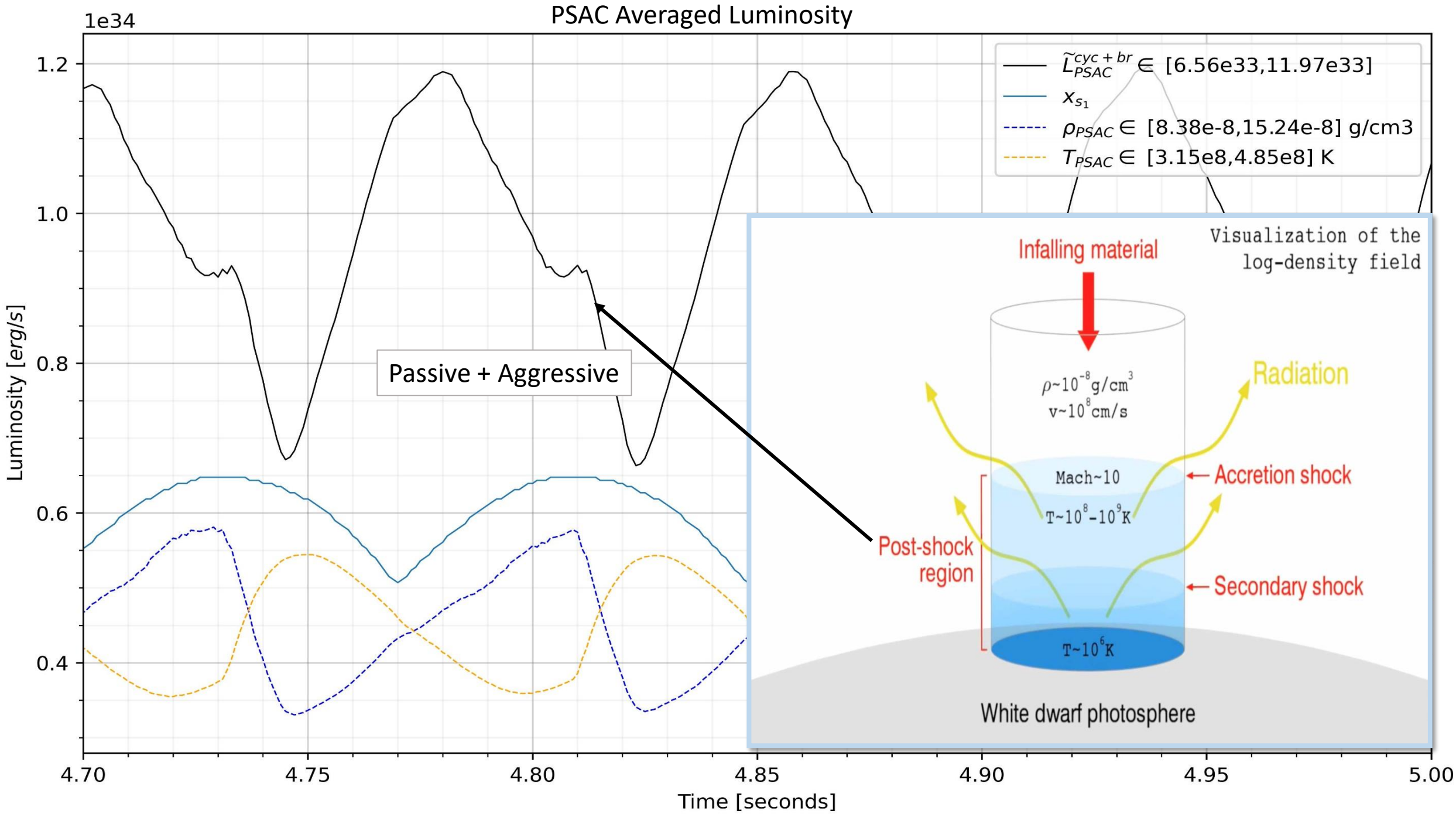
PSAC Averaged Luminosity
1e34
1.2
1.0
0.8
0.6
0.4
Luminosity [erg/s]
4.70
4.75
4.80
4.85
4.90
4.95
5.00
Time [seconds]
$\widetilde{L}^{cyc+br}_{PSAC} \in$ [6.56e33,11.97e33]
x_{s_1}
$\rho_{PSAC} \in$ [8.38e-8,15.24e-8] g/cm3
$T_{PSAC} \in$ [3.15e8,4.85e8] K
Passive + Aggressive
Visualization of the log-density field
Infalling material
ρ~10^{-8}g/cm^3
v~10^8cm/s
Radiation
Mach~10
T~10^8-10^9K
Accretion shock
Post-shock region
Secondary shock
T~10^6K
White dwarf photosphere

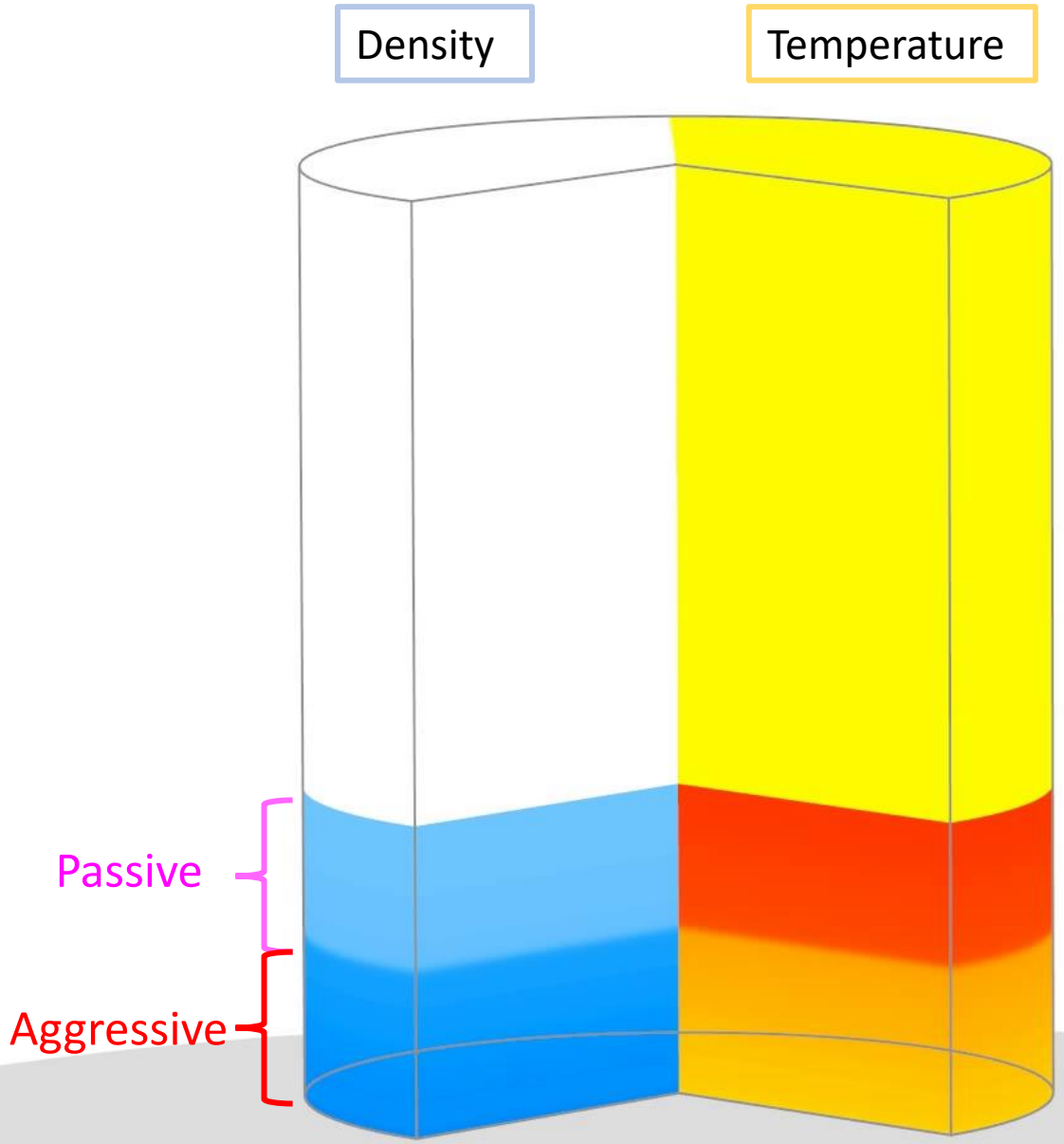

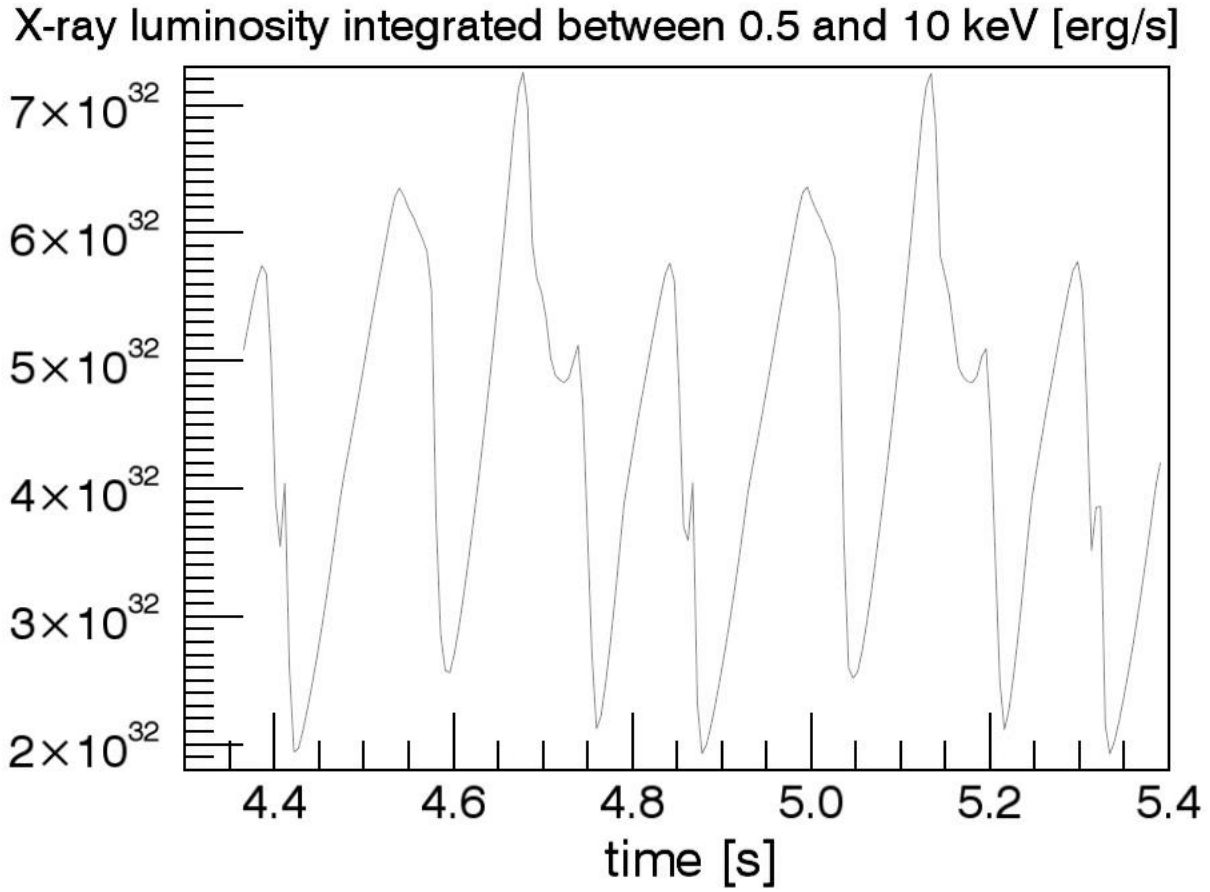

White dwarf photosphere

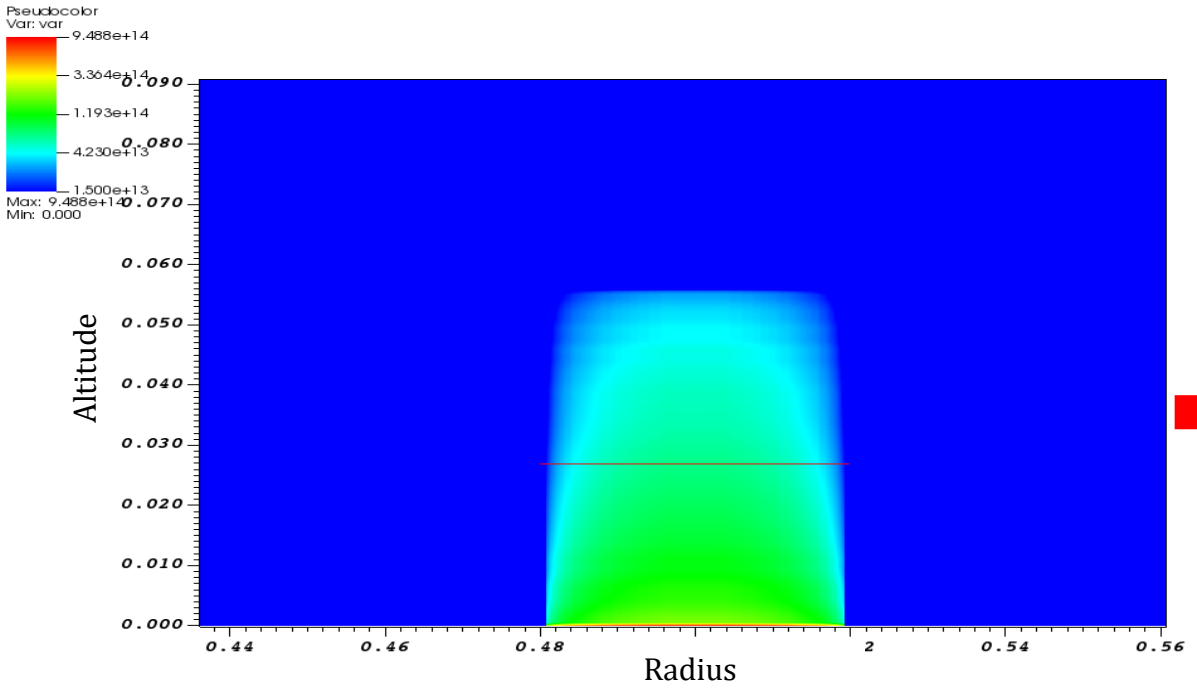
Pseudocolor
Var: var
9.488e+14
3.364e+14
1.193e+14
4.230e+13
1.500e+13
Max: 9.488e+14
Min: 0.000
Altitude
Radius

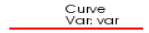
Curve
Var: var

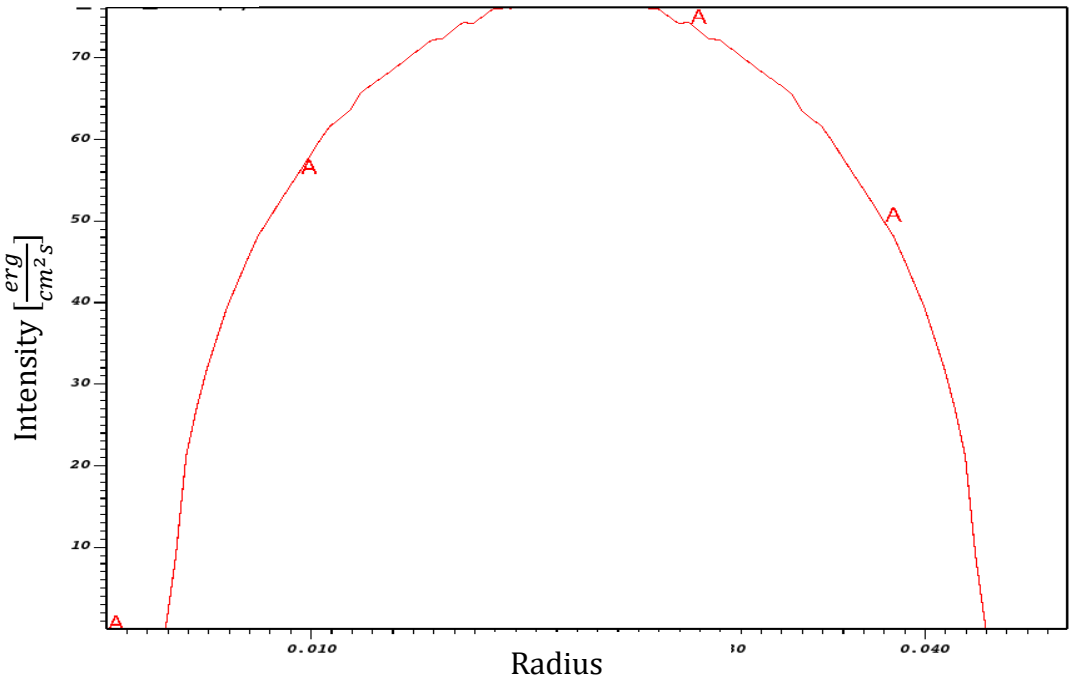
Intensity $[\frac{erg}{cm^2 s}]$
Radius

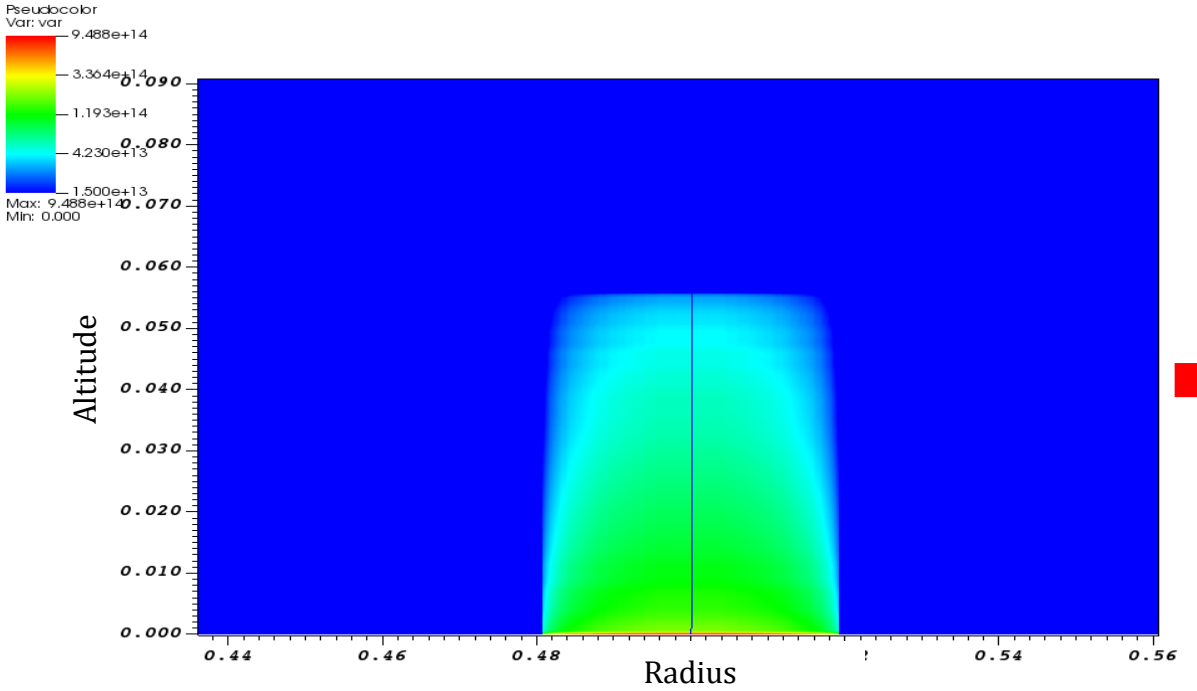
Pseudocolor
Var: var
9.488e+14
3.364e+14
1.193e+14
4.230e+13
1.500e+13
Max: 9.488e+14
Min: 0.000
Altitude
Radius

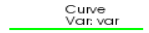
Curve
Var: var

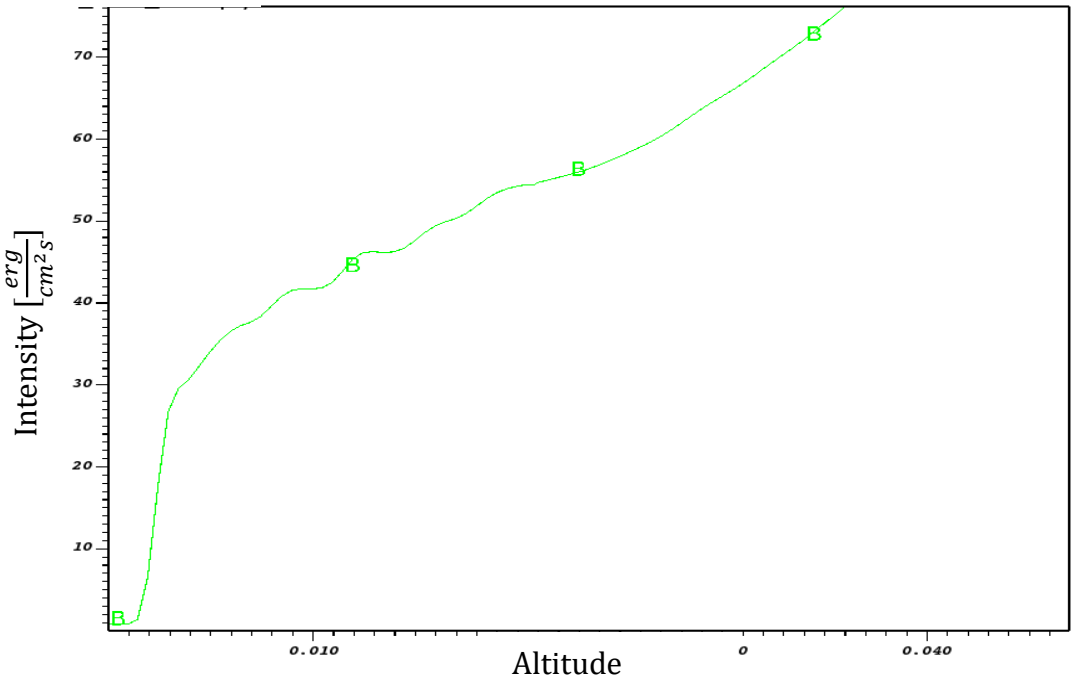
Intensity $[\frac{erg}{cm^2 s}]$
Altitude

IMPROVEMENTS?

Further stability analysis of compressional forces and cooling forces at different altitudes.

Cooling role over time w.r.t. energy reservoir.

Addition of magnetic effects.

Implementation of blobs, segmented and non-steady accretion flow.

Testing agreement with observation and laboratory laser experiments.

THANK YOU